LA-9956-MS, Part 1

Los Alamos National Laboratory is operated by the University of California for the United States Department of Energy under contract W-7405-ENG-36.

Losses in Magnetic Flux Compression Generators, Part I: Linear Diffusion

Los Alamos
Los Alamos National Laboratory
Los Alamos, New Mexico 87545

LA 9956-MS, Part 1

ERRATA

p 12 Delete colon, line 2.

p 17 Eqs (2.28) and (2.29). Replace x limits (x and ∞) by λ.

p 18 Eqs (2.31) and (2.32). Add = SE on right hand sides, for clarity of argument. Eq (2.33), replace ES by SE.

p 47 Lines 8 and 9 from bottom. Interchange Eqs (5.18) and (5.17) in text.

p 58 Eq (5.42). Argument s of exponent $-R\tau/Lo$ is omitted at start of right hand side.

Sect. 5.5 Two R's used inadvertently. Through Eq (5.44), R is resistance. In Eqs (5.45) - (5.47), R is Reynolds No. except in the combination $2R\tau/L_o$, Eq. (5.45), where it is resistance.

LA-9956-MS, Part 1

UC-38
Issued: February 1984

Losses in Magnetic Flux Compression Generators, Part 1: Linear Diffusion

C. M. Fowler

Los Alamos National Laboratory
Los Alamos, New Mexico 87545

LOSSES IN MAGNETIC FLUX COMPRESSION GENERATORS, PART 1: LINEAR DIFFUSION

by

C. M. Fowler

ABSTRACT

This is the first of three monographs devoted to a detailed analysis of magnetic flux losses in explosive-driven flux compression generators. Magnetic field diffusion into generator conductors can lead to substantial losses. A study of linear diffusion is therefore the major subject treated in this report. Diffusion analysis is considerably complicated by the presence of moving conductors and the compression of magnetic flux. Consequently the text is treated in a tutorial fashion. This is particularly true in the earlier parts of the report where formulation of basic equations, various conservation laws, and problem solutions are treated in considerable detail. A point of departure from earlier treatments of the subject is the addition of external circuits to the generators. It is shown that the influence of these circuits enters into the boundary conditions for the diffusion equations. A number of new analytic solutions are obtained for various external circuits.

---

1. INTRODUCTION

This is the first of three reports whose purpose is to consider in more detail some of the electromagnetic phenomena associated with explosive-driven magnetic flux compression generators. A primer that treated these devices in a

general manner was published in 1975 by Fowler, Caird, and Garn.[1] As with the great bulk of other work published on these generators, the associated analytic treatment was carried out with lumped parameter models. The authors referred the readers to other works for more extensive analyses, such as the diffusion of magnetic fields into conducting elements of the generators. An understanding of this diffusion is extremely important as the process can lead to substantial generator losses. Consequently, two of the three reports, including this one, deal with diffusion. As usual, the wave nature of the electromagnetic effects is suppressed. The other report of this series includes wave phenomena, which then allow a better understanding of the electromagnetic losses through the boundaries of generator conductors.

The subject of this report is one-dimensional linear magnetic diffusion. Unlike the diffusion treatments normally encountered, including heat conduction, the presence of moving boundaries and compression of flux greatly complicates the situation. Only a very few analytic solutions have been obtained previously. These solutions, together with several new ones, are included here. Most of the solutions are obtained by Laplace transformation techniques, some of them not often encountered. I have tried to make the text tutorial in nature. Consequently, the earlier problems, in particular, are treated here in detail--considerably more than would appear in a journal article, for example. In this regard, I have chosen to write solutions mainly in terms of the Bromwich contour integral rather than using the symbol L^{-1} for the inverse of the transforms. Partly, this is because additional integrations are required for some solutions but also because the symbol, L, for inductance, occurs many times in the text.

A class of explosive flux compression devices called plate generators serves as the vehicle for the text examples. Figure 1 is a schematic drawing that shows a cross-sectional view of the generator and a cylindrical load coil. The solid lines are metallic conductors. The active volume of the generator is bounded by the rectangular section, whose upper and lower faces (plates) are adjacent to the high-explosive slabs. The cylindrical load coil is connected in series to the generator by a short transmission line.

The generator system works in the following way. Initial magnetic flux is first developed in the generator working volume. This is accomplished either by a capacitor discharge through the system (as indicated on Fig. 1) or by induction through an external coil system. When capacitor banks are used, ini-

tial flux is also developed in the load coil. The explosive slabs are initiated at such a time that the generator current input slot is closed off (through motion of the top plate) at or near the time when maximum initial flux is developed. The flux is now confined completely by metallic conductors. As time progresses, the top and bottom plates move inward as shown for one instant of time on Fig. 1 by the dashed lines. The flux is therefore compressed into a region of lower inductance with a consequent increase in current and magnetic energy.

The plate generator should have its greatest application to low-inductance systems where large current and power delivery are required. The power level is controlled in part by the speed at which the generator volume is wiped out. With use of light-weight plates, such as dural, we have achieved velocities approaching 5 km/s. With two convergent plates, as shown in Fig. 1, the relative plate speed approaches 10 km/s. For a given generator, the current-carrying capacity is limited by the width of the conductors, in this case perpendicular to the cross-sectional view of Fig. 1.

The plate generator concept is not new,[2] and we have used generators of this type in one form or another for many years. The generator plate dimensions formerly were limited by the size of suitable plane explosive initiation systems. However, a few years ago a new initiation system was developed at Los Alamos that had no inherent limitations on the area it could initiate. This led to significant advances in both size and versatility of the generators.[3]

Normally, the performance of a generator-powered circuit is obtained from the solution of lumped parameter equations. As an example, a single equation, Eq. (1.1), represents the system shown on Fig. 1.

$$\frac{d}{dt}\left[L_G(t)I\right] + IR + L_1\frac{dI}{dt} + L^1\frac{dI}{dt} = 0 \; ; \qquad I(0) = I_0 \; . \tag{1.1}$$

Here, $L_G(t)$ is the inductance of the generator, which changes with time under explosive action, I is the current flowing through the system, L_1 is the inductance of the cylindrical load coil and L^1 is the stray or source inductance in the system. I_o is the initial value of the current in the system at the start of plate motion, i.e., the time when the top plate closes off the feed current

input slot. This also removes the capacitor bank from any further interaction with the system. Allowance is made for the nonperfect conductivity of the system by insertion of the resistive term, IR, in the equation. Values of R are generally assigned so that the analytic solutions agree most closely with experimental results.

The generator inductance is presumed to be known as a function of the time. If the length ℓ and width w of the plate generator of Fig. 1 are much greater than the plate separation, 2x, the inductance of the generator can be written:

$$L = \mu\ell \cdot \frac{2x}{w} \quad . \tag{1.2}$$

After a short acceleration period, the generator plate speeds level off to an approximately constant velocity. Thus, if the initial plate separation is $2x_0$ and the average plate velocity is v, we can approximate the time-varying generator inductance by

$$L = \mu\ell \frac{2(x_0 - vt)}{w} \quad . \tag{1.3}$$

An equivalent expression is

$$L = L_0 \left(1 - \frac{t}{\tau}\right) ; \qquad L_0 = \frac{2\mu\ell x_0}{w} ; \qquad \tau = \frac{x_0}{v} \quad . \tag{1.4}$$

In the discussion to follow, the plate generator inductance will be represented by the expressions given in Eqs. (1.3) or (1.4). As will be seen later, use of this approximate form greatly simplifies the analysis but still allows investigation of the salient features.

Evaluation of the source or stray inductance, L^1, of Eq. (1.1) is the major objective of this study. As it turns out, one of the major losses in generator-powered systems resides in the flux trapped in the so-called "skin"

of the metal conductors. This flux, which increases during generator action, is normally not retrievable after burnout. A realistic evaluation of the skin depths requires magnetic diffusion theory.

To illustrate the contents of this report and to point out areas of departure from previous work in magnetic diffusion, consider Fig. 2. Formally, this system is equivalent to that shown on Fig. 1, whose performance is represented by Eq. (1.1), in which part of the resistance and source inductance is estimated for the generator. In the class of problems we take up here, lumped parameters are employed in the external circuitry, but complete space-time variables are used for the generator plates. This is our major point of departure from past work, which is, to our knowledge, devoted entirely to studies aimed at establishing values of maximum magnetic fields attainable from flux compression devices with no external circuitry.

Knoepfel,[4] in his book Pulsed High Magnetic Fields, surveys previous work in magnetic field diffusion. Paton and Millar[5] as well as Lehner, Linhart, and Somon[6] present analytic solutions to the plane compression problem.

The organization of this report is as follows:

In Sec. 2, Maxwell's equations are adapted to the plane diffusion problem, boundary conditions are defined, the energy balance equation for nonlinear diffusion problems is set forth, and expressions for effective plate resistance, skin depth, and flux loss are developed.

In Sec. 3, new closed-form solutions are obtained for the linear problem (constant conductivity) and fixed- (nonmoving-) plane-bounded cavities coupled to external lumped circuits. It is shown here how the ordinary differential

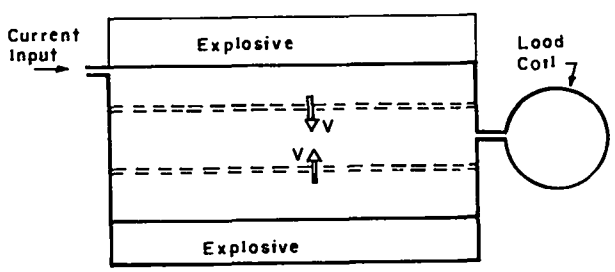

Fig. 1.
Schematic drawing of a plate generator with external load coil.

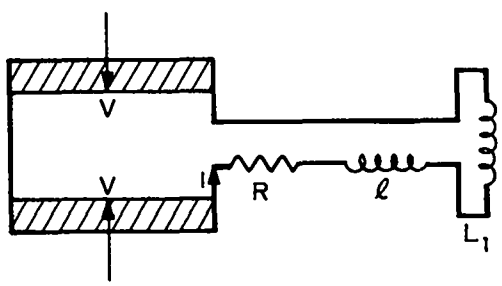

Fig. 2.
External circuit elements attached to plate generator output.

equations encountered in lumped circuit analysis appear as boundary conditions to the diffusion equations.

Lumped parameter solutions to simple systems, such as shown in Fig. 1, are developed in Sec. 4 mainly for comparison with the more extensive solutions developed later.

Moving-plate problems are treated in Sec. 5, where new closed-form solutions are presented for several linear cases.

Finally, brief discussions of some recent, or newly discovered, works are given in the Appendix.

2. BASIC EQUATIONS

The essential elements of the class of problems in which we are interested are illustrated in Fig. 2. For the most part, the generator is taken as symmetric about a center-plane between the two slabs, and our analysis then is restricted to only one of the two planes.

The external circuitry shown on the figure can be generalized in any required manner with the understanding that it is handled by means of lumped parameters and engineering circuit theory. There may be any number of coupled circuits, switches, etc., but for each branch, the various circuit elements are represented by lumped resistances, capacitances, inductances, etc. A single total current is considered to adequately represent charge flow in each branch. In other words, Kirchhoff's laws are considered to apply. A number of simplifying restrictions are required to obtain reasonably manageable solutions which embody the diffusion aspects of the slab walls.

(i) The slabs are treated as incompressible. For the cases of most interest to us, that is, when the slabs function as moving walls for a generator, the instantaneous velocities of every element in the slabs are equal. This greatly simplifies the electromagnetic analysis in that only a single instantaneous velocity is required throughout the moving medium. In fact, this allows us to handle the moving medium as stationary in all respects for first-order accuracy and throw the entire burden of accounting for the motion onto the $\overline{v} \times \overline{B}$ voltage developed at the boundary.

(ii) Although much of the work set forth in this report can be carried further with variable instantaneous slab velocities, most of the questions in which we are interested can be elucidated by assuming the slab velocities are constant. In view of the resulting great reduction in complexity, we will take the slab velocities as constant for the generator problems to be considered later.

(iii) The slab material will be treated as isotropic. Electrical conductivity and later thermal conductivity, will be considered to be scalars. The conductivities may be functions of temperature or deposited energy, but they are independent of direction or hysteresis effects. The permeability and susceptibilities are taken as constants, and further, when the situations arise, free space values are usually employed, although this is not required.

(iv) Only the single Cartesian space variable, x, is employed in the analysis. As will be seen later, magnetic skin depths are generally quite small. Parts of the analysis should therefore be applicable to other non-planar systems except for regions of large curvature, such as the later stages of cylindrical compression. The length and width of the plates are assumed to be much larger than plate spacings or thicknesses to justify the one-dimensional treatment. Clearly, the analysis will not account for the tendency of currents to build up near the edges of conductors as a

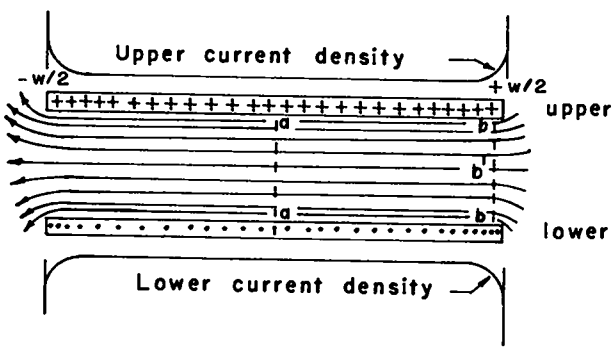

Fig. 3.
Illustration of current concentration at conductor edges.

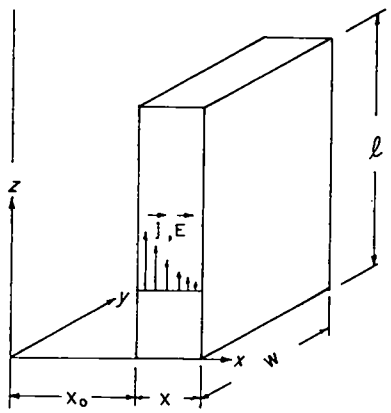

Fig. 4.
Coordinates and slab dimensions employed in text.

means of uniformizing the flux contained under each current-carrying element of the conductor, such as shown in Fig. 3.

When a total current I flows in good conducting parallel plates of finite width, w, (into the upper plate, and out of the lower plate) the current density is not uniform. Rather, there is a pile-up of current near the ends of the plate ($\pm$ w/2) in such a manner as to generate a constant flux along the width of the conductor. Across the central plane, aa, the magnetic field is nearly uniform. Near the conductor edges, such as the plane bb, the fields near the plates are larger and those in the mid-region, b′, smaller than the nearly uniform values in the plane aa. The total fluxes in both planes are nearly the same. If the current density was uniform, the total flux would be smaller at bb′b than at aa, approaching only half the value as the widths became very great compared to the spacing.

This flux-distributing effect of good conductors is most pronounced for systems when the width and spacing are comparable. In this case, fields actually existing in the central region may be 10-20% smaller than the values calculated based upon an assumed uniform current distribution. This two-dimensional effect cannot, of course, be treated here. However, the effect is not large if the lateral dimensions are several times larger than the x-dimensions that are significant. In fact, for most of the practical systems developed here, another two-dimensional effect is of at least comparable significance. This effect is the natural lagging near the edges of explosively propelled plates, which also must be ignored here.

2.1 Standard Slab Geometry.

Figure 4 is a sketch of one of the two slab faces. Coordinates are standard Cartesian, x corresponding to position in the slab. Current densities and electric fields are in the z-direction, slab motion in the negative x-direction, and magnetic fields will be in the negative y-direction. The slab length, ℓ, in the direction of the currents, and the width, w, are both large enough that edge effects are considered negligible as discussed previously.

Maxwell's equations and Ohm's law take the following forms:

$$\nabla \times \vec{E} = -\frac{\partial \vec{B}}{\partial t} \quad , \tag{2.1}$$

$$\nabla \times \vec{B} = \mu \vec{j} + \frac{1}{c^2} \frac{\partial \vec{E}}{\partial t} \quad , \text{ and} \tag{2.2}$$

$$\vec{j} = \sigma \vec{E} \equiv \frac{1}{\rho} \vec{E} \quad . \tag{2.3}$$

As noted earlier, the wave nature of the fields is considered in another report. Here, the displacement current of Eq. (2.2) is neglected. The scalar resistivity (inverse of the conductivity) may depend upon other variables. We now assume that all field quantities depend upon time, t, and the single space variable, x, and write

$$\vec{j} = j(x,t)\ \vec{c} \quad , \tag{2.4}$$

$$\vec{E} = E(x,t)\ \vec{c} \quad , \text{ and} \tag{2.5}$$

$$\overline{B} = B(x,t)\ \vec{b} \quad . \tag{2.6}$$

The unit Cartesian vectors ($\vec{a}$, $\vec{b}$, $\vec{c}$) do not appear elsewhere in this report. Equations (2.1)-(2.3) then reduce to the following:

$$\frac{\partial E}{\partial x} = \frac{\partial B}{\partial t} \quad , \text{ and} \tag{2.7}$$

$$\frac{\partial B}{\partial x} = \mu j = \mu \sigma E = \frac{\mu}{\rho} E \quad . \tag{2.8}$$

As is well known, under the conditions of constant velocity, the Maxwell's equations for a moving slab reduce to those for a stationary slab (to first-order corrections in slab velocity relative to that of light) with the addition of motional electric fields at the boundary. More generally, the electric field generated by changing magnetic fields, Eq. (2.1), for moving

conductors gives rise to motional potentials around a circuit given by the total change in flux encompassed by the circuit. This potential, added to any other potential sources in the circuit, gives the total potential drop across the circuit as measured by an observer fixed with respect to the external circuitry. Thus, in Fig. 2 the potential appearing across the leads to the external circuitry arises from resistive drops along the generator plates and from changes in magnetic flux bounded by the plates.

A precise accounting of the transient fields both between the slabs and outside them will be given in the second report of this series. However, in the spirit of the diffusion equation approximation for the slab, we also neglect displacement currents for the free space regions adjacent to the slabs. This is equivalent to assuming a spatially uniform but time-varying magnetic field in the region between the two conducting slabs.[7] From Eq. (2.1), the interslab electric field varies linearly with distance between the slabs. The amplitude is set by values of E at the slab boundaries, and the time behavior is governed by the cavity magnetic field time behavior.

Because the permeability of the slabs is taken as that of vacuum (not a necessary restriction here), the magnetic fields are continuous across the slab boundaries. Thus, the magnetic fields at the inner slab boundaries, $B(0,t)$, are equated to the interslab cavity field.

We can also show that in the absence of externally impressed magnetic fields on the slab system, the magnetic fields on the outer slab boundaries are zero in the diffusion equation approximation. Before showing this and deriving other relationships of interest, we take up the question of the algebraic sign of the magnetic field. The cross sections of the two symmetric slabs are shown on Fig. 5 at one instant of time. Our subsequent analysis will be carried out only on the right slab, where $x > o$, since proper attention to symmetry will eliminate the need for further consideration of the left slab. Shown plotted across the slabs in solid lines are curves representing the current density. In our subsequent analysis, at least initially, we will consider the current density as positive in the right-hand slab. The current densities in the left-hand, or return slab, are then negative. At the time t_1, current densities are plotted for both slabs. On the right-hand slab, the current density is also plotted for a later time, t_2. (In generator problems, the currents normally increase with time.) The electric fields differ from the current densities only by the conductivity factor, σ, according to Eq. (2.3).

The magnetic fields must appear qualitatively as sketched in Fig. 5 with dashed lines, for they must increase negatively in time, from Eq. (2.7), but have positive space derivatives, from Eq. (2.8). Further, from Stokes theorem and Eq. (2.2), or more specifically, Eq. (2.8), the line integral of the magnetic field which encloses both conductors must be zero. Symmetry then demands that the magnetic fields must be zero on the outer slab boundaries.

The total current, I, flowing through the slab of width w, and thus through external circuitry as well, is the areal integral of the current density:

$$I = w\int_0^{\lambda} j(x,t)\, dx \quad . \tag{2.9}$$

Here, as in most tractable problems, we are able to shift the slab origin to zero. The slab thickness is λ, which we will take to be infinite in most cases.

Integration of Eq. (2.8) with $B(\lambda,t) = 0$ yields the results

$$B(x,t) = -\frac{\mu}{w} I(t) + \mu\int_0^{x} j(x,t)\, dx \quad , \text{ and} \tag{2.10}$$

$$B(0,t) = B_{cavity} = \frac{-\mu}{w} I(t) \quad . \tag{2.11}$$

Equation (2.11) is particularly significant in that it relates the cavity field to the total current flowing through the system and further shows that we must assign opposite signs to the current and the magnetic field.

The magnetic field diffusion equation follows from Eqs. (2.7) and (2.8):

$$\frac{\partial B}{\partial t} = \frac{\partial}{\partial x}\left(\frac{\rho}{\mu}\right)\frac{\partial B}{\partial x} \quad . \tag{2.12}$$

The solution of this equation under various conditions forms the basis of most of this report. Some quantities of interest are the following:

(i) Magnetic skin depth, D_{sk}. This quantity is defined at any instant of time as that depth in the slab: which, when multiplied by the inner boundary, or cavity, field gives the flux in the slab.

$$D_{sk}(t) \equiv \int_0^{\lambda} \frac{B(x,t)\, dx}{B(0,t)} \quad . \tag{2.13}$$

(ii) Flux leakage. Integration of Eq. (2.12) over the slab gives

$$\frac{\partial}{\partial t}\int_0^{\lambda} B(x,t)\, dx = \int_0^{\lambda} \frac{\partial}{\partial x}\left(\frac{\rho}{\mu}\right)\frac{\partial B}{\partial x}\, dx, \text{ or}$$

$$\frac{\partial \phi_{slab}}{\partial t} = \left(\frac{\rho}{\mu}\ \frac{\partial B}{\partial x}\right)_{\lambda} - \left(\frac{\rho}{\mu}\ \frac{\partial B}{\partial x}\right)_0 \quad . \tag{2.14}$$

The interpretation of Eq. (2.14) is clear. The quantity ϕ_{slab} is the flux per unit length residing in the slab. Its increase with time is given by the difference of the two terms at its boundaries. Flux enters the slab at the inside boundary and leaves at the outer boundary:

$$\left(-\frac{\rho}{\mu}\frac{\partial B}{\partial x}\right)_{0,\lambda} = \text{rate of flux leakage into and out of slab per unit length.} \tag{2.15}$$

We have mentioned that the potential drop across the inner slab faces consists of the term $-(d\phi/dt)$ enclosed by the slabs as well as other terms such as resistive drops along the slabs. We consider here the resistive term. Equation (2.8) relates the electric field at the slab boundary to the boundary magnetic field gradient. If the slab lengths are ℓ, the resistive drop across the two slabs, $2E(0,t)\ell$, becomes

$$V_{res} = 2\ell \left(\frac{\rho}{\mu}\frac{\partial B}{\partial x}\right)_{x=0} \quad . \tag{2.16}$$

(iii) Effective slab resistance, R_{sq}. Frequently we are interested in an effective resistance per square for the slabs. We set the above expression equal to IR and eliminate I through Eq. (2.11) to obtain:

$$R = -\frac{2\ell}{w} \frac{\left(\rho \frac{\partial B}{\partial x}\right)_{x=0}}{B(0,t)} .$$

Since $2\ell/w$ is the number of slab squares in the generator, we obtain for the resistance per square, R_{sq}:

$$R_{sq} = -\frac{\left(\rho \frac{\partial B}{\partial x}\right)_{x=0}}{B(0,t)} . \qquad (2.17)$$

For very thin slabs, we show later that both ρ and $\partial B/\partial x$ are independent of x. In this case the resistance per square is reduced to ρ/λ, where λ is the thickness of the slab. For thick slabs, if the spatial variation of B is exponential, with e-folding distance δ, R_{sq} reduces to ρ/δ. It is clear, however, that difficulties may be encountered with this definition, for example, if the cavity field gets very small or reverses signs.

2.2 Resistivity Variations

Considerable simplification in calculation is achieved by limiting the variation of resistivity to linear variations with temperature. The form for resistivity we have chosen is then given by Eq. (2.18), where α is constant:

$$\rho(T) = \rho_0 \left[1 + \alpha(T-T_0)\right] . \qquad (2.18)$$

Thermal conductivity effects are shown to be small in a later report. Consequently, they are ignored here and the heating effects are then assumed to arise only from energy deposition from the currents flowing in the conductors. Thus the temperature rise in time Δt is given by

$$DC\ \Delta T = j^2 \rho\ \Delta t \quad . \tag{2.19}$$

Here, D is the density of the conductor, and C is the specific heat. We replace the current density by the magnetic field gradient, from Eq. (2.8), eliminate the temperature from Eq. (2.18), and work with the normalized resistivity, r:

$$r = \frac{\rho}{\rho_0} \quad , \text{ and} \tag{2.20}$$

$$\frac{\partial r}{\partial t} = \frac{\alpha \rho_0}{\mu^2 DC}\, r\, \left(\frac{\partial B}{\partial x}\right)^2 \quad . \tag{2.21}$$

In the third report of this series, we assume that initially the slabs are at constant resistivity ρ_0 throughout and that the density and heat capacity are constant. It then becomes convenient to lump the constant terms in Eq. (2.21) together and rewrite this equation as follows:

$$\frac{\partial r}{\partial t} = Kr\, \left(\frac{\partial B}{\partial x}\right)^2 \; ; \quad K = \frac{\alpha \rho_0}{DC\mu^2} \quad . \tag{2.22}$$

2.3 Collection of Equations

The dependent variables are the magnetic field B(x,t), the normalized resistivity r(x,t), and the total current I, related to the inner slab boundary, or cavity field, Eq. (2.11).

The partial differential equations are Eq. (2.21) for r(x,t), and, in terms of the normalized resistivity, r, we rewrite Eq. (2.12) as follows for the magnetic field diffusion equation:

$$\frac{\partial B}{\partial t} = \frac{\rho_0}{\mu}\ \frac{\partial}{\partial x}\left(r\, \frac{\partial B}{\partial x}\right) \quad . \tag{2.23}$$

The initial conditions generally are given by $r(x,0) = 1$ and $B(x,0) = 0$. There are no boundary conditions on r.

At the outer slab boundary, the magnetic field is zero: $B(\lambda,t) = 0$.

The inner slab boundary condition is derived by making the total potential drop around the slabs and any connected external circuitry equal to zero. The potential drop around the slabs consists of the negative rate of change of flux enclosed by the slabs and the resistive drop along the slabs of Eq. (2.16). The boundary condition is then given by the following equation, where ρ has been replaced by the normalized resistivity:

$$-\frac{d\phi_{cavity}}{dt} + \frac{2\ell\rho_0}{\mu}\left(r\,\frac{\partial B}{\partial x}\right)_{x=0} + V_{ext} = 0 \quad . \tag{2.24}$$

For the linear problems of constant conductivity, the solutions are usually developed in terms of the constant conductivity, $\sigma = 1/\rho_0$. The applicable equations then become

$$\frac{\partial B}{\partial t} = \frac{1}{\mu\sigma}\,\frac{\partial^2 B}{\partial x^2} \quad , \text{ and} \tag{2.25}$$

$$-\frac{d\phi_{cavity}}{dt} + \frac{2\ell}{\mu\sigma}\left(\frac{\partial B}{\partial x}\right)_{x=0} + V_{ext} = 0 \quad . \tag{2.26}$$

A few solutions to the linear problem, Eqs. (2.25) and (2.26), are given in Sec. 3 and illustrate how external circuitry enters as a boundary condition to the diffusion equation. For these examples, the slabs will be taken as stationary.

2.4 Energy Balance

It is shown first that the Poynting flux into the two slab faces accounts for the magnetic field energy and heat dissipation in the slabs. In a first example with fixed slab boundaries, it is then shown that this energy is at the expense of the initial cavity magnetic field energy. Then, the moving slab geometry with external circuitry is considered. It is shown that additional energy supplied to the system arises from the well-known lumped parameter generator power term, $I^2\dot{L}/2$. The analysis is given for arbitrary temperature variation of the slab resistivity.

The electric field is given by Eq. (2.8). The energy input, PE, to the two slabs from the Poynting flux, $\overline{E} \times \overline{H}$, is then given by

$$PE = \frac{-2\ell w \rho_0}{\mu^2} \int_0^t \left(rB \frac{\partial B}{\partial x} \right)_{x=0} dt \quad . \tag{2.27}$$

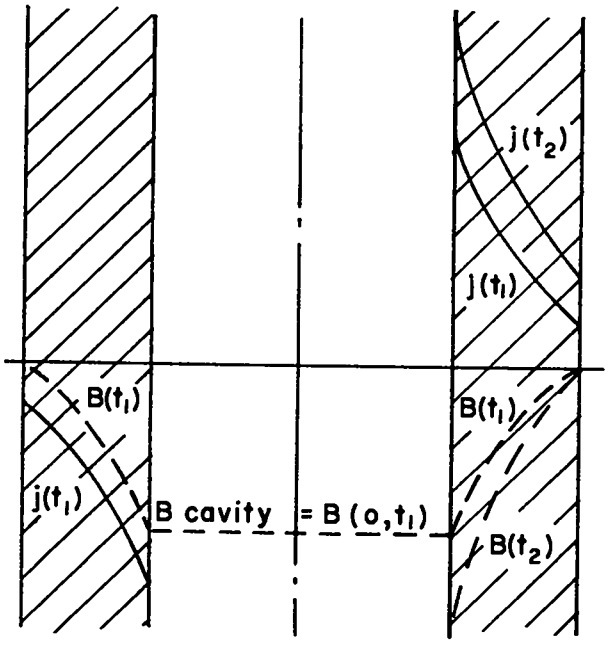

Fig. 5.
Comparison of slab current densities and magnetic fields at two different times.

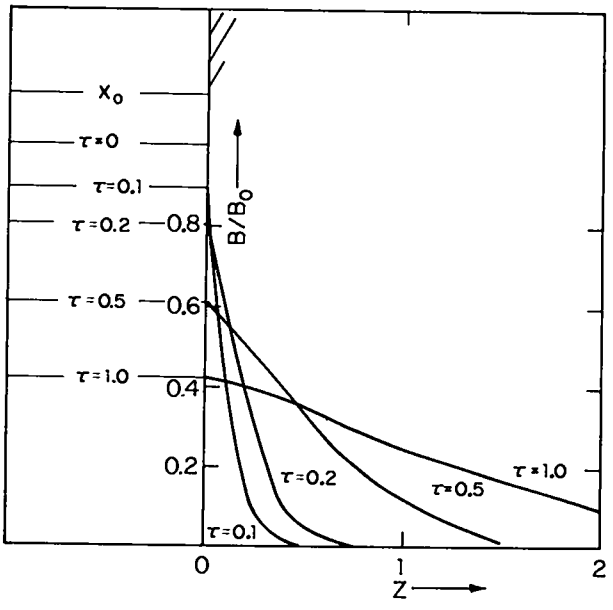

Fig. 6.
Magnetic field diffusion from a cavity into semi-infinite slabs. Total flux is conserved.

The energy dissipated as heat is obtained by integrating $j^2\rho$ over the slab volumes and time. We obtain j from Eq. (2.8) and get for the energy deposited in the slabs, SE, including the magnetic energy,

$$SE = 2\ell w\int_0^{\infty} \frac{B^2(x,t)}{2\mu}dx + \frac{2\ell w\rho_0}{\mu^2}\int_0^t\int_0^{\infty} r\left(\frac{\partial B}{\partial x}\right)^2 dxdt \quad . \tag{2.28}$$

Differentiation of this expression after time followed by parts integration of the last term yields the expression

$$\frac{2\ell w}{\mu}\left[\int_0^x B\frac{\partial B}{\partial t}\,dx + \frac{\rho_0}{\mu} r\frac{B\partial B}{\partial x}\Big/_0^{\infty} - \int_0^x \frac{\rho_0 B}{\mu}\frac{\partial}{\partial x}\frac{(r\partial B}{\partial x})\,dx\right] \quad . \tag{2.29}$$

The integral terms vanish, from Eq. (2.12), and the remaining term evaluated at x=0 is just the integrand of Eq. (2.27). Thus, the Poynting flux from the cavity supplies both the magnetic and thermal energies resident in the slabs.

Further deductions can be made by linking the Poynting flux to the slab boundary condition, Eq. (2.24). As a first example, we consider stationary slabs with an initial cavity field B_0 and no external circuitry. The cavity flux is then $2x_0\ell B(0,t)$. The space derivative in Eq. (2.27) may now be eliminated by using the boundary condition. Integration then yields

$$PE = 2\ell w x_0[B_0^2 - B(0,t)^2]/2\mu \quad . \tag{2.30}$$

Therefore the Poynting energy, which supplies energy to the slabs, arises from the loss of magnetic energy in the cavity. In other words total energy is conserved.

We now consider the general boundary condition, which includes an external potential source and allows for slab motion. Eliminating the field space derivatives from Eq. (2.24), the Poynting energy becomes

$$PE = -2\int_0^t \frac{wB(0,t)}{2\mu}\left(\frac{d\phi}{dt}\text{ cavity}-V_{ext}\right)dt \quad . \tag{2.31}$$

The cavity flux is $2x\ell B(0,t)$. We replace $B(0,t)$ by the current I, Eq. (2.11), and replace x with the cavity inductance, $L = 2\mu\ell x/w$, to obtain

$$PE = -\int_0^t \left[I\frac{d(LI)}{dt} + IV_{ext}\right]dt \quad . \tag{2.32}$$

Rearrangement of Eq. (2.32) yields the equation

$$\int_0^t -\frac{1}{2} I^2 \frac{dL}{dt}\, dt = \frac{1}{2} LI^2 - \frac{1}{2} L_0 I^2{}_0 + \int_0^t V_{ext}\, I\, dt + ES \quad . \tag{2.33}$$

The left integral is the power that must be supplied to change the cavity inductance. This power supplies the slab energy, both magnetic and thermal, energy delivered to the external circuitry, and increases in the magnetic energy stored in the cavity.

3. PROBLEMS OF CONSTANT CONDUCTIVITY, STATIONARY SLABS

In this section we obtain the solution to several problems where the conductivity is constant and the slabs are stationary and of infinite extent in the x-direction. In the first example, no external circuitry is employed. To the author's knowledge, this is the only example of the many treated here for which a closed-form solution has been obtained.[8] The remaining problems have external circuitry attached to the slabs and serve mainly as examples in management of the boundary conditions. Solutions in this section and in Sec. 5, where the slabs move, are obtained by Laplace transform methods. The Table of Laplace Transforms, by Roberts and Kaufman,[9] and The Handbook of Mathematical Functions, edited by Abramowitz and Stegun,[10] have been found to be quite useful.

3.1 No External Circuitry.

In this case, the initial slab separation, $2x_0$ is constant, and the flux in the cavity is given by

$$\phi_{cav} = 2x_0 \, \ell \, B(0,t) \quad .$$

There is no external potential, V_{ext}, in Eq. (2.26). Equations (2.25) and (2.26) are then restated together with appropriate initial conditions as follows:

$$\frac{\partial B}{\partial t} = \frac{1}{\mu\sigma} \frac{\partial^2 B}{\partial x^2} \quad , \tag{3.1}$$

$$- 2x_0 \, \ell \frac{dB(0,t)}{dt} + \frac{2\ell}{\mu\sigma} \left(\frac{\partial B}{\partial x}\right)_0 = 0 \quad , \tag{3.2}$$

$$B(x,0) = 0 \quad , \tag{3.3}$$

$$B(0,0) = B_0 \quad , \text{ and} \tag{3.4}$$

$$B(\infty,t) = 0 \quad . \tag{3.5}$$

According to Eqs. (3.3) and (3.4), the initial magnetic field B_0 resides only in the cavity between the slabs. From Eq. (2.11) it follows that an initial total current I_0 of magnitude $-w \, B_0/\mu$ flows on the inner slab surfaces.

Normally, when the current I is used as the dependent variable, it is taken to be positive. In this example, the magnetic field is taken as the dependent variable, and the sign of the fields will be that of B_0. No confusion should arise as long as it is recognized that the signs of the current densities, electric fields, and total current, if needed, must carry signs opposite to that of B_0.

Before solving Eqs. (3.1)-(3.5), we point out that the boundary condition, Eq. (3.2), is equivalent to stating that the rate at which magnetic energy leaves the cavity is given by the Poynting flux into the cavity walls. The magnetic energy in the cavity is given by

$$\varepsilon_{cav} = \frac{B_0^2(0,t)}{2\mu} \cdot 2x_0 \, \ell w \quad ,$$

and its rate of leakage is then

$$\frac{d\varepsilon_{cav}}{dt} = \frac{B_0(0,t)}{\mu} \frac{\partial B(0,t)}{\partial t} \cdot 2x_0 \, \ell w \quad .$$

The Poynting flux into the two walls, $2\ell w(EH)_0$ from Eq. (2.8), is then

$$(EH)_0 \cdot 2 \, \ell w = \frac{1}{\mu\sigma} \left(\frac{\partial B}{\partial x}\right)_0 \cdot \frac{B(0,t)}{\mu} \cdot 2 \, \ell w \quad .$$

Equation of the two expressions leads to Eq. (3.2).

To solve Eqs. (3.1)-(3.5), we let $\beta(x,s)$ be the Laplace transform of $B(x,t)$.

$$\beta(x,s) = \int_0^\infty e^{-st} \, B(x,t) \, dt \quad . \tag{3.6}$$

Multiplication of Eq. (3.1) by e^{-st} followed by time integration yields the results

$$B(x,t) \, e^{-st} \Big|_0^\infty + s \int_0^\infty e^{-st} \, B(x,t) \, dt \quad , \text{ and}$$

$$= \frac{1}{\mu\sigma} \frac{d^2}{dx^2} \int_0^\infty B(x,t) \, e^{-st} \, dt \quad .$$

Using Eq. (3.3) we obtain

$$\frac{d^2\beta}{dx^2} = \mu\sigma s\beta \quad . \tag{3.7}$$

Multiplication of Eq. (3.2) by e^{-st} followed by time integration yields

$$- 2x_0 \ell \left[B(0,t)\ e^{-st}\ \right]_0^\infty + s\int_0^\infty B(0,t)\ e^{-st}\ dt$$
$$+ \frac{2\ell}{\mu\sigma}\ \frac{d}{dx}\int_0^\infty B(x,t)\ e^{-st}\ dt\ \Big|_{x=0} = 0 \quad . \tag{3.8}$$

Thus, with Eq. (3.4) the inner boundary condition becomes

$$\frac{1}{\mu\sigma x_0}\left(\frac{d\beta}{dx}\right)_0 - s\ \beta(0,s) + B_0 = 0 \quad . \tag{3.9}$$

Equation (3.5) yields the result that $\beta(_\infty,s) = 0$. The solution to Eq. (3.7) satisfying this condition is

$$\beta(x,s) = A(s)\ e^{-x\sqrt{\mu\sigma s}} \quad . \tag{3.10}$$

Substitution of Eq. (3.10) into Eq. (3.9) allows calculation of A(s), and the solution for $\beta(x,s)$ becomes

$$\beta(x,s) = \frac{B_0\ e^{-x\sqrt{\mu\sigma s}}}{s + \frac{1}{x_0}\sqrt{s/\mu\sigma}} \quad . \tag{3.11}$$

Thus, the solution for B(x,t) is given by the inverse transform of $\beta(x,s)$:

$$B(x,t) = L^{-1}[\beta(x,s)] = \frac{B_0}{2\pi i} \int_{Br} \frac{e^{st - x\sqrt{\mu\sigma s}}\, ds}{s + \frac{1}{x_0}\sqrt{s/\mu\sigma}} \quad . \tag{3.12}$$

Before setting down the solution to this integral, we also derive expressions for the flux. The flux in the cavity is given by $2x_0\ \ell B(0,t)$. That in the two slabs is given by $2\ell\int_0^\infty B(x,t)\, dx$. Expressions for these terms follow from Eq. (3.12):

$$\phi_{cav} = 2x_0\ \ell B_0 \frac{1}{2\pi i} \int_{Br} \frac{e^{st}\, ds}{s + \frac{1}{x_0}\sqrt{s/\mu\sigma}} \quad , \text{ and} \tag{3.13}$$

$$\phi_{slabs} = 2B_0\ \ell \frac{1}{2\pi i} \int_{Br} \frac{e^{st}\, ds}{\sqrt{\mu\sigma s}\left(s + \frac{1}{x_0}\sqrt{s/\mu\sigma}\right)} \quad . \tag{3.14}$$

The appropriate inverse transforms for these terms are given in Ref. 9 [Eqs. (28) and (30), p. 248]. The solutions are:

$$B(x,t) = B_0 \exp\left(\frac{x}{x_0} + \frac{t}{\mu\sigma x_0^2}\right) \operatorname{Erfc}\left(\frac{1}{x_0}\sqrt{t/\mu\sigma} + \frac{x}{2}\sqrt{\mu\sigma/t}\right) \quad , \tag{3.15}$$

$$\phi_{cav} = 2B_0\ x_0\ \ell \exp\left(\frac{t}{\mu\sigma x_0^2}\right) \operatorname{Erfc}\left(\frac{1}{x_0}\sqrt{t/\mu\sigma}\right) \quad , \text{ and} \tag{3.16}$$

$$\phi_{slabs} = 2B_0\ x_0\ \ell \left[1 - \exp\left(\frac{t}{\mu\sigma x_0^2}\right) \operatorname{Erfc}\left(\frac{1}{x_0}\sqrt{t/\mu\sigma}\right)\right] \quad . \tag{3.17}$$

Equations (3.16) and (3.17) show that the total flux in the cavity and slabs is conserved (equal to the initial flux $2B_0\ x_0\ \ell$) as it should be. Had the slab thickness, λ, been finite, then, even though $B(\lambda,t) = 0$, the space derivative there would not vanish. Flux would leak out of this boundary

according to Eq. (2.15), and the total flux in the cavity and slabs would not be conserved.

Equation (3.15) can be rewritten in terms of normalized space and time parameters, z and τ, as follows:

$$z = \frac{x}{x_0} \; ; \qquad \tau = \frac{1}{x_0} \sqrt{t/\mu\sigma} \tag{3.18}$$

$$\frac{B(z,\tau)}{B_0} = \exp(z + \tau^2) \; \mathrm{Erfc}\left(\tau + \frac{z}{2\tau}\right) \; . \tag{3.19}$$

Plots of $B(z,\tau)/B_0$ are given on Fig. 6 for both cavity and slab position for various values τ with use of tabulated values of the complementary error function.

Some idea of the flux leakage rates may be obtained as follows. Generally speaking, slab conductors have conductivities of order $3\text{-}5.10^7$ mho/m, and cavity dimensions are of the order of some centimeters. Times of interest are usually in the microsecond range. If we set $\sigma = 4 \times 10^7$, $x_0 = 0.05$ m, and $t = 50$ μs, we find $\tau = 0.02$. From Fig. 6 we see that very little flux has leaked out of the cavity at this time. If the cavity were only 2 cm wide ($x_0 = 0.01$ m), at a time of 200 μs, $\tau = 0.2$, and approximately 20% of the flux has leaked into the slabs from the cavity.

The slab skin depth, D_{sk}, can also be obtained from Fig. 6 in terms of the cavity fields. Since total flux is conserved, $2x_0B_0 = (2x_0 + 2\,D_{sk})\,B$, and

$$D_{sk} = x_0(B_0/B-1) \; .$$

For small values of time, expansion of Eq. (3.19) shows that $B(0,\tau)/B_0 \doteq 1-2\tau/\sqrt{\pi}$. For large values of time the asymptotic expansion, from Ref. 10 [Eq. (7.1.23), p 298], is $B(0,\tau)/B_0 \doteq 1/\tau\sqrt{\pi}$. With Eq. (3.18), the skin depth becomes

$$D_{sk} \doteq 2(t/\pi\mu\sigma)^{1/2}, \text{ small } t;$$

$$D_{sk} \doteq \pi(t/\pi\mu\sigma)^{1/2}, \text{ large } t.$$

3.2 External Inductance, L_1

In this example, an external load of fixed inductance L_1 is hooked across the slab outputs, such as shown on Fig. 2. The external potential across this inductance is given by

$$\frac{d}{dt}(L_1 I) = L_1 \frac{dI}{dt} \quad . \tag{3.20}$$

Here, I is the total current flowing through the slabs and external circuit. We again formulate our equations in terms of magnetic fields. Use of Eq. (2.11) then gives

$$V_{L_1} = V_{ext} = -\frac{wL_1}{\mu}\frac{dB(0,t)}{dt} \quad . \tag{3.21}$$

Substitution of this expression in Eq. (2.26) gives

$$-2x_0 \ell \frac{dB(0,t)}{dt} + \frac{2\ell}{\mu\sigma}\left(\frac{\partial B}{\partial x}\right)_0 - \frac{wL_1}{\mu}\frac{dB(0,t)}{dt} = 0 \quad . \tag{3.22}$$

This equation replaces Eq. (3.2) of the previous example for the inner slab boundary condition. The other equations of the set, Eqs. (3.1)-(3.5), remain the same. The solution to the problem proceeds exactly as before except for calculation of the coefficient A(s) of Eq. (3.10), which is now obtained from Eq. (3.22). The solution for A(s) differs only in that the parameters $1/\mu\sigma x_0$ is changed. Previously it was obtained from Eq. (3.8), from the ratio of the terms $2\ell/\mu\sigma$ and $2x_0\ell$. In this example, it is obtained from the ratio of $2\ell/\mu\sigma$ and $(2x_0\ell + wL_1/\mu)$. Noting that the cavity inductance $L_0 = 2\mu x_0 \ell/w$, we have the following solution for A(s) and B(x,t)

$$A(s) = \frac{B_0}{s + \frac{L_0}{L_1 + L_0}\frac{1}{x_0}\sqrt{s/\mu\sigma}} \quad , \text{ and} \tag{3.23}$$

$$B(x,t) = \frac{B_0}{2\pi i}\int_{Br} \frac{e^{st-\sqrt{\mu\sigma s}\,x}\,ds}{s + \frac{L_0}{L_0 + L_1}\frac{1}{x_0}\sqrt{s/\mu\sigma}} \quad . \tag{3.24}$$

The solutions, Eq. (3.15)-(3.17), obtained from the preceding example may be taken over directly with the replacement of x_0 by $x_0[(L_0 + L_1)/L_0]$. Thus, we can use the normalized solution, Eq. (3.19), for the slab fields (and the cavity field, $z = 0$), by setting

$$z = \frac{x}{x_0(L_0+L_1)/L_0} \quad ; \quad \tau = \frac{\sqrt{t/\mu\sigma}}{x_0(L_0+L_1)/L_0} \quad . \tag{3.25}$$

It is seen from Eq. (3.25) that the addition of the external inductance to the cavity has the effect of lowering τ. Thus, the flux leakage rate from the cavity is reduced by the addition of an external inductance. This is not surprising since the external inductance carries the same current as the slabs and therefore functions as a ballast.

Finally, we note that conservation of flux in the system must now include that in the external inductance in addition to that in the cavity and slabs. Using the proportionality of current and cavity field, we have for the initial flux in the system

$$\phi_0 = (L_0 + L_1)\frac{w}{\mu}B_0 \quad . \tag{3.26}$$

At later times, the flux in the cavity, slabs, and external inductance is

$$\phi(t) = 2\ell\, x_0\, B(0,t) + 2\ell \int_0^{\infty} B(x,t)\, dx + \frac{w}{\mu} L_1\, B(0,t) \quad . \tag{3.27}$$

We now use Eqs. (3.13) and (3.14), replacing x_0 by $x_0[(L_0 + L_1)/L_0]$, to obtain

$$\phi(t) = B_0\left(2x_0\ell + \frac{wL_1}{\mu}\right) \cdot \frac{1}{2\pi i} \int_{Br} \frac{e^{st}\, ds}{s + \dfrac{L_0}{L_0 + L_1}\, \dfrac{1}{x_0}\sqrt{s/\mu\sigma}}$$

$$+ 2B_0\ell \cdot \frac{1}{2\pi i} \int_{Br} \frac{e^{st}\, ds}{\left(s + \dfrac{L_0}{L_0 + L_1}\, \dfrac{1}{x_0}\sqrt{s/\mu\sigma}\right)\sqrt{\mu\sigma s}}$$

$$= \frac{B_0 w}{\mu} \cdot \frac{1}{2\pi i} \int_{Br} \frac{e^{st}\, ds}{s + \dfrac{L_0}{L_0 + L_1}\, \dfrac{1}{x_0}\sqrt{s/\mu\sigma}} \left(L_0 + L_1 + \frac{2\ell\mu\, x_0}{x_0\, w\, \sqrt{\mu\sigma s}}\right);$$

$$\phi(t) = \frac{B_0 w}{\mu}(L_0 + L_1) \cdot \frac{1}{2\pi i} \int_{Br} \frac{e^{st}\, ds}{s} = \frac{B_0 w}{\mu}(L_0 + L_1) \quad . \tag{3.28}$$

As is well known, the value of the integral along the Bromwich contour is $2\pi i$. Thus, the total flux at any time equals the initial flux of Eq: (3:26): With this result the skin depth can be obtained from Eq. (3.27) since the integral term is equal to $2D_{sk}\, B(0,t)$.

$$D_{sk} = x_0(B_0/B(0,t)-1)(L_0 + L_1)/L_0 \quad .$$

Equations (3.19) and (3.25) show that the skin depth for both very small and very large values of time are the same as those given in Sec. 3.1, where there was no external inductance. However, since the values of τ are smaller in the present case, the cavity field has not decreased as much in the same time.

3.3 External Inductance and Resistance

Figure 2 again serves as a schematic for this situation, with the conducting slabs taken as stationary and of infinite thickness. As before, an initial surface current I_0 of magnitude $-B_0(w/\mu)$ flows through the slabs and external circuitry, which now includes the resistance R in addition to the inductance L_1 of the previous example.

The term V_{ext} of Eq. (2.24) must now include the IR potential drop as well as the term $L_1(dI/dt)$ used in the previous example. Again, we eliminate I through use of Eq. (2.11) and write the boundary condition in terms of the cavity field, B(0,t). Equation (2.24) then becomes

$$- 2x_0 \ell \frac{dB(0,t)}{dt} + \frac{2\ell}{\mu\sigma} \left(\frac{\partial B}{\partial x}\right)_0 - R \frac{w}{\mu} B(0,t) - \frac{w}{\mu} L_1 \frac{dB(0,t)}{dt} = 0 \quad . \qquad (3.29)$$

Using the expression $L_0 = 2x_0 \mu\ell/w$ for the cavity inductance, we can rearrange this equation as follows:

$$- \frac{dB(0,t)}{dt} - \frac{R}{L_0 + L_1} B(0,t) + \frac{L_0}{L_0 + L_1} \cdot \frac{1}{\mu\sigma x_0} \left(\frac{\partial B}{\partial x}\right)_0 = 0 \quad . \qquad (3.30)$$

Except for Eq. (3.2), which this equation replaces, the set of Eqs. (3.1)-(3.5) remains the same. The solution proceeds as in Sec. 3.1, and we determine A(s) from the transform of Eq. (3.30). We obtain this transform as before, by multiplying the equation by e^{-st} and integrating after time.

$$- \int_0^\infty e^{-st} \frac{dB(0,t)}{dt} dt - \frac{R}{L_0 + L_1} \int_0^\infty e^{-st} B(0,t)\, dt$$

$$+ \frac{L_0}{L_0 + L_1} \cdot \frac{1}{\mu\sigma x_0} \frac{\partial}{\partial x} \int_0^\infty B(x,t)\, e^{-st}\, dt \Big|_0 = 0 \quad . \qquad (3.31)$$

The result is, with Eq. (3.4),

$$\frac{L_0}{L_0 + L_1} \frac{1}{\mu\sigma x_0} \left(\frac{d\beta}{dx}\right)_0 = \beta \left(s + \frac{R}{L_0 + L_1}\right) - B_0 \quad . \tag{3.32}$$

Substitution of Eq. (3.10) into this expression allows the determination of A(s):

$$A(s) = \frac{B_0}{s + \frac{R}{L_0 + L_1} + \frac{L_0}{L_0 + L_1} \frac{1}{x_0} \sqrt{s/\mu\sigma}} \quad . \tag{3.33}$$

The solution for B(x,t) then becomes

$$\begin{aligned} B(x,t) &= L^{-1} \left[A(s)\, e^{-\sqrt{\mu\sigma s}\, x}\right] \\ &= \frac{B_0}{2\pi i} \int_{Br} \frac{e^{st - x\sqrt{\mu\sigma s}}\, ds}{s + \frac{R}{L_0 + L_1} + \frac{L_0}{L_0 + L_1} \frac{1}{x_0} \sqrt{s/\mu\sigma}} \quad . \end{aligned} \tag{3.34}$$

When R = 0, we note that this equation correctly reduces to Eq. (3.24), which is the solution for the case when the external load is purely inductive.

We are usually most interested in the total current flowing in the system, which we write in terms of the cavity field, B(0,t). We can then write

$$I(t) = I_0 \frac{1}{2\pi i} \int_{Br} \frac{e^{st}\, ds}{s + \frac{R}{L_0 + L_1} + \frac{L_0}{L_0 + L_1} \frac{1}{x_0} \sqrt{s/\mu\sigma}} \quad . \tag{3.35}$$

We can reduce Eq. (3.35) to an integral form as follows. We note that the function whose inverse transform we seek is the reciprocal of a quadratic function in $s^{1/2}$:

$$g(s^{1/2}) = \frac{I_0}{(s^{1/2})^2 + \frac{L_0}{L_0 + L_1} \frac{1}{x_0 \sqrt{\mu\sigma}} (s^{1/2}) + \frac{R}{L_0 + L_1}} \quad . \tag{3.36}$$

According to Ref. 9 [Eq. (29), p. 171], if f(u) is the inverse transform of g(s), then the inverse transform of $g(s^{1/2})$ is given as follows:

$$L^{-1}[g(s^{1/2})] = \frac{1}{2\sqrt{\pi t^3}} \int_0^\infty u\, e^{-u^2/4t}\, f(u)\, du \quad . \tag{3.37}$$

The function f(u) is now the inverse transform of a simple rational expression:

$$f(u) = \frac{I_0}{2\pi i} \int_{Br} \frac{e^{su}\, ds}{s^2 + \alpha s + \beta} \quad . \tag{3.38}$$

$$\alpha = \frac{L_0}{L_0 + L_1} \frac{1}{x_0 \sqrt{\mu\sigma}} ; \qquad \beta = \frac{R}{L_0 + L_1} \quad . \tag{3.39}$$

The roots of the quadratic $s^2 + \alpha s + \beta$ for typical plate generators will be complex. For example, if $L_0 = 0.09$ μH, $L_1 = 0.01$ μH, $x_0 = 0.05$ m, $\sigma = 10^7$ mho/m, and $R = 0.001$ Ω, then

$$\alpha \doteq 5 , \qquad \beta = 10^4 ,$$

and the discriminant $\alpha^2/4 - \beta$ is negative. From Ref. 9 [Eq. (152), p. 199] we obtain

$$f(u) = I_0\, e^{-\alpha u/2}\, \frac{\sin\left[u\left(\beta - \frac{\alpha^2}{4}\right)^{1/2}\right]}{\left(\beta - \frac{\alpha^2}{4}\right)^{1/2}} \quad . \tag{3.40}$$

From Eq. (3.37), we obtain

$$I(t) = \frac{I_0}{2t^{3/2}\left[\pi\left(\beta - \frac{\alpha^2}{4}\right)\right]^{1/2}}$$

$$\times \int_0^\infty u\, du\, e^{-u^2/4t - (\alpha u/2)}\, \sin u\left(\beta - \frac{\alpha^2}{4}\right)^{1/2} \quad . \tag{3.41}$$

We note that if the slabs were perfectly conducting, $\sigma \to \infty$, then $\alpha = 0$. Under these conditions, Eq. (3.41) reduces to

$$I(t) = \frac{I_0}{2t^{3/2}\sqrt{\beta\pi}} \int_0^\infty u\, du\, e^{-u^2/4t}\, \sin(\sqrt{\beta}\, u) \; ; \quad \sigma = \infty \quad . \tag{3.42}$$

With the help of Ref. 10 [Eq. (7.4.6), p. 302], this expression is easily shown to reduce to the following:

$$I(t) = I_0\, e^{-\beta t} \equiv I_0\, e^{-Rt/(L_0+L_1)} \; ; \quad \sigma = \infty \quad . \tag{3.43}$$

This is the elementary solution obtained for the current decay in a circuit of resistance R and inductance $L_0 + L_1$, as expected, since the perfect conductivity of the slabs prevents field diffusion into them, and the cavity then behaves as a pure inductance of value L_0. Incidentally, Eq. (3.43) follows immediately from Eq. (3.35) when the conductivity is infinite.

Equation (3.41) can be expressed in terms of tabulated functions as follows. For convenience we set $\gamma = (\beta - \alpha^2/4)^{1/2}$ temporarily and integrate Eq. (3.41) by parts to obtain

$$I(t) = \frac{I_0}{\gamma \sqrt{\pi t}} \int_0^\infty e^{-(u^2/4t)\ -(\alpha u/2)}$$

$$\times\, du \left(-\frac{\alpha}{2} \sin \gamma u + \gamma \cos \gamma u\right) \quad . \tag{3.44}$$

From Ref. 9[Eq. (7.4.2), p. 302] we have

$$\int_0^\infty e^{-(ay^2+2by)}\, dy = \frac{1}{2} \sqrt{\pi/a}\ e^{+b^2/a}\ \mathrm{Erfc}(b/\sqrt{a}) \ ;\ R\ell a > 0 \quad . \tag{3.45}$$

Upon replacing sin γu and cos γu by their exponential equivalent expressions, Eq. (3.44) can be put in the form of two definite integrals having the form of Eq. (3.45), with complex coefficients, b. We obtain

$$I(t) = \frac{I_0}{2\gamma} \left[\left(\gamma + \frac{i\alpha}{2}\right) e^{t[(\alpha/2)-i\gamma]^2}\ \mathrm{Erfc}\ \sqrt{t}\ \left(\frac{\alpha}{2} - i\gamma\right) + \mathrm{C.C.}\right] \quad . \tag{3.46}$$

This reduces to the following:

$$I(t) = \frac{I_0}{2\gamma \sqrt{t}} \left[z\, e^{-z^2}\ \mathrm{Erfc}(-iz) + \mathrm{C.C.}\right] \quad , \tag{3.47}$$

where

$$z = \sqrt{t}\ \left(\gamma + \frac{\alpha i}{2}\right) \equiv \left[\left(\beta - \frac{\alpha^2}{4}\right)^{1/2} + i\,\frac{\alpha}{2}\right] \sqrt{t} \quad . \tag{3.48}$$

From Ref. 10 [Eq. (7.1.3), p. 297] we note first that Eq. (3.47) can be expressed in terms of a function w(z) related to error functions of complex

arguments. This function is also tabulated in Ref. 10 [Table 7.9, p. 325]. We finally have

$$I(t) = \frac{I_0}{\gamma \sqrt{t}} R\ell \, [z \, w(z)] \quad . \tag{3.49}$$

If the slabs are perfectly conducting, $\alpha = 0$, $\gamma = \sqrt{\beta}$, and $z = \sqrt{\beta t}$ is real. From Ref. 10 [Eq. (7.1.3), p. 297] we then obtain, again, the result given in Eq. (3.43) for this limiting case.

It can be shown that when $\alpha^2 << \beta$, i.e., the slabs are very good conductors, then the diffusion effects are small, and I(t), given by Eq. (3.49), is approximately that given in Eq. (3.43). When α^2 is comparable to β (poor slab conductivity or slab cavity dimensions very small), then diffusion effects perturb seriously the lumped parameter solution, Eq. (3.43). As an example, let us take the following parameters:

$$\beta = 10^4 \; ; \qquad \alpha = 120 \; ; \qquad t = 10^{-4}\tau \quad .$$

The lumped parameter solution Eq. (3.43) becomes

$$\frac{I(\tau)}{I_0} = e^{-\tau} \quad . \tag{3.50}$$

The solution with diffusion taken into account reduces to

$$\frac{I(\tau)}{I_0} = R\ell \left\{ \frac{1}{0.8} (0.8 + 0.6i) \, w\left[\sqrt{\tau} \, (0.8 + 0.6i)\right] \right\} \quad . \tag{3.51}$$

These two solutions, the latter obtained from the tables of Ref. 10, are compared on Fig. 7 together with a few additional points calculated from

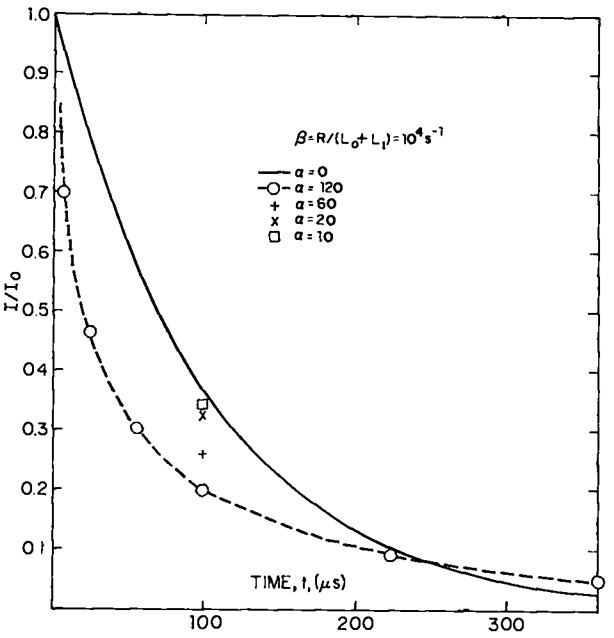

Fig. 7.
Current decay in an external circuit connected to a slab-bounded cavity showing influence of diffusion. The upper curve is a lumped parameter solution without diffusion.

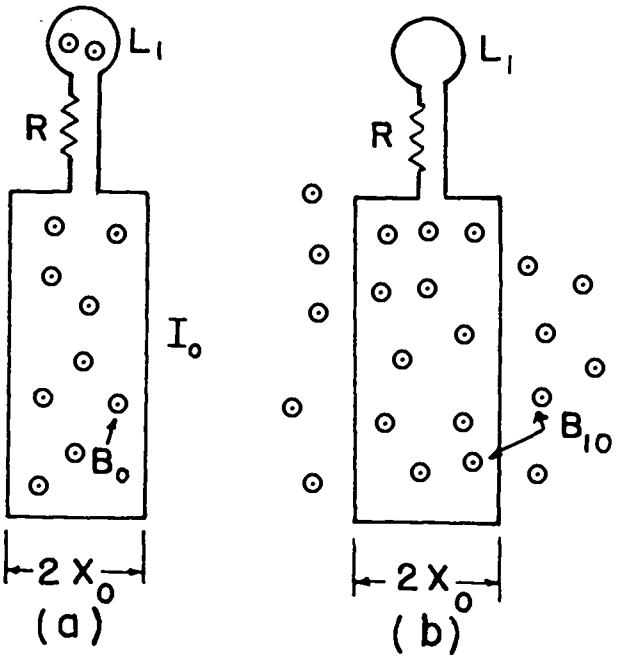

Fig. 8.
Two ways of producing flux in a conductor-bounded cavity (a) by discharging a current directly through the conductors (b) from an external magnetic field source.

Eq. (3.49) that show how the solution approaches the lumped parameter solution as the slab conductivity increases.

3.4 External Capacitance

Figure 2 serves as a sketch to illustrate this example. As before, the slabs are stationary and of infinite extent in the x-direction. Here, the external load is a capacitor with capacitance C and initial voltage V_0. Unlike the preceding examples, current starts to flow through the system only after C is switched into the circuit, at time t = 0. The external potential, V_{ext}, of Eq. (3.36) becomes

$$V_{ext} = V_0 + \frac{1}{C}\int_0^t I\, dt \quad . \tag{3.52}$$

Replacing the external current by the cavity field, the boundary condition, Eq. (2.26), which replaces Eq. (3.2) of example (3.1), becomes

$$-2\,x_0\,\ell\,\frac{dB(0,t)}{dt} + \frac{2\ell}{\mu\sigma}\left(\frac{\partial B}{\partial x}\right)_0 + V_0 - \frac{w}{\mu C}\int_0^t B(0,t)\,dt = 0 \quad . \tag{3.53}$$

Equation (3.4) is simplified since the initial cavity field is zero. With this condition, the Laplace transform of Eq. (3.53) becomes (with the help of Ref. 9 [Eq. (41), p. 7, n = 1]

$$-2x_0 s\ell\,\beta(s,0) + \frac{2\ell}{\mu\sigma}\left(\frac{d\beta}{dx}\right)_0 + \frac{V_0}{s} - \frac{w\beta(0,s)}{\mu C s} = 0 \quad . \tag{3.54}$$

As before, from Eqs. (3.1), (3.3), and (3.5), the acceptable solution for $\beta(x,s)$ is given by Eq. (3.10), where A(s) is now determined from Eq. (3.54), and $\beta(x,s)$ becomes

$$\beta(x,s) = \frac{V_0\, e^{-\sqrt{\mu\sigma s}\,x}}{2x_0\,\ell\,s^2 + \frac{2\ell}{\sqrt{\mu\sigma}}\,s^{3/2} + \frac{w}{\mu C}} \quad . \tag{3.55}$$

B(x,t) is then

$$B(x,t) = L^{-1}[\beta(x,s)] = \frac{V_0}{2\pi i}\int_{Br} \frac{e^{st - x\sqrt{\mu\sigma s}}\,ds}{2x_0\,\ell\,s^2 + \frac{2\ell}{\sqrt{\mu\sigma}}\,s^{3/2} + \frac{w}{\mu C}} \quad . \tag{3.56}$$

The expression for the total current in the system, $I(t) = -(w/\mu)\,B(0,t)$, becomes, with use of the expression $L_0 = 2\mu\,x_0\,\ell/w$,

$$I(t) = -\frac{V_0}{L_0}\frac{1}{2\pi i}\int_{Br}\frac{e^{st}\,ds}{s^2 + \frac{1}{x_0\sqrt{\mu\sigma}}s^{3/2} + \frac{1}{LC}} \quad . \tag{3.57}$$

It is of interest to compare this result with the corresponding lumped parameter solution with a resistance R in the circuit:

$$I(t) = -\frac{V_0}{L_0}\frac{1}{2\pi i}\int_{Br}\frac{e^{st}\,ds}{s^2 + \frac{R}{L}s + \frac{1}{LC}} \quad . \tag{3.58}$$

The well-known solution of Eq. (3.58) is

$$I(t) = -\frac{V_0}{L_0\omega}e^{-(R/2L)t}\sin\omega t \; ; \qquad \omega = \left[\frac{1}{LC} - \left(\frac{R}{2L}\right)^2\right]^{1/2} \quad . \tag{3.59}$$

Equations (3.57) and (3.58) become identical when the circuits are lossless, $\sigma = \infty$, $R = 0$, and the solution, from Eq. (3.59), reduces to

$$I(t) = -V_0\sqrt{C/L}\sin\omega t \; ; \quad \omega = (LC)^{-1/2} \; ; \quad \sigma = \infty \quad . \tag{3.60}$$

When the conductivity is large, the resistive term in Eq. (3.57) should be small, and the poles of s are in magnitude, close to ω. Upon comparison with Eq. (3.58), we would expect the term $\omega^{1/2}/x_0\sqrt{\mu\sigma}$ to be somewhat comparable to the term R/L, where R is an effective resistance for the slabs. If we express the slab resistance in terms of an effective skin depth, τ_{eff}, we find

$$\tau_{eff} = (\mu\sigma\omega)^{-1/2} \quad . \tag{3.61}$$

This expression agrees with the classical skin depth for an oscillating boundary field of frequency ω to within a factor $\sqrt{2}$.

Equation (3.57) can be expressed analytically, but the solution requires that the roots be obtained of the quartic expression (in $s^{1/2}$) of the denominator of the integral. The algebra required to do this is extensive and we have not done so. However, some solutions that were obtained by numerical techniques will be given in the third report of this series.

4. LUMPED PARAMETER SOLUTIONS

Solutions to flux compression problems are usually carried out with use of lumped parameters. Diffusion effects are approximated by adding external resistances and inductances that are treated as loss terms. A fairly detailed account of this treatment may be found in Ref. 1.

We take up here some of these solutions for the plate generator. There are two objectives to this study. The first objective is to introduce the techniques required to obtain the boundary equations for moving slabs. These will be carried over to the diffusion treatment of moving slabs given in Sec. 5.

The second objective is to compare solutions to the plate generator problem when the initial cavity flux is obtained from (a) an initial current flowing through the system or when it is obtained from (b) a magnetic field derived from external sources. The solutions differ somewhat, and the difference also carries over to the diffusion treatment for the same problems as will be pointed out in Sec. 5.

4.1 Initial Flux and Circuit Equations

Figure 8 shows the two methods of supplying initial flux to the slab cavity. In both cases, there is an external load consisting of an inductance L_1 and resistance R. In Fig. 8a, initial flux is produced by an initial current, I_0, flowing through the system. The magnetic field arising from this current, $-\mu I_0/\omega$, is confined to the slab cavity. In Fig. 8b, the initial field, B_{10}, is impressed on the cavity from an external source. In the diffusion equation solutions to be discussed in Sec. 5, the source must be of infinite extent to be consistent with Maxwell's equations. No initial currents

flow in this system. The circuit equations and solutions are carried out in parallel below.

As the slabs start to move inwards, the flux is compressed. In case (a), I_0 increases. In case (b), a current starts to flow through the system. We obtain the circuit equations from Eq. (2.26). For both cases, the external potentials and flux terms are given by

$$V_{ext} = IR + L_1 \frac{dI}{dt} \quad , \text{ and} \tag{4.1}$$

$$\phi = 2x\, \ell\, B_{cavity} \quad . \tag{4.2}$$

For case (a), the cavity field arises solely from the current. In case (b), it arises not only from the current but from the externally impressed field B_{10}. Thus,

$$\phi = - \frac{2x\ell\mu I}{w} = - LI \quad , \text{ and} \qquad \text{(a)} \tag{4.3}$$

$$\phi = 2x\ell \left(B_{10} - \frac{\mu I}{w}\right) = 2x\ell B_{10} - LI \quad . \qquad \text{(b)} \tag{4.4}$$

Combining these equations with Eq. (4.1), we obtain the differential equations for the two cases from Eq: (2:26):

$$\frac{d}{dt}(LI) + IR + L_1 \frac{dI}{dt} = 0 \; ; \quad I(0) = I_0 \qquad \text{(a)} \tag{4.5}$$

$$\frac{d}{dt}(LI - 2x\ell\, B_{10}) + IR + L_1 \frac{dI}{dt} = 0 \; ; \quad I(0) = 0 \quad . \qquad \text{(b)} \tag{4.6}$$

For purposes of simplification, we may replace the initial magnetic field B_{10} by an effective current I_{10}:

$$I_{10} = -\frac{wB_{10}}{\mu} \quad . \tag{4.7}$$

We can consolidate Eqs. (4.5) and (4.6) to

$$\frac{d}{dt}(L + L_1)\, I + IR = 0 \; ; \quad I(0) = I_0 \qquad \text{(a)} \tag{4.8}$$

$$\frac{d}{dt}\left[(L + L_1)(I + I_{10})\right] + IR = 0 \; ; \quad I(0) = 0 \quad . \qquad \text{(b)} \tag{4.9}$$

Although Eq. (4.8) was derived for the slab geometry, it is used in practice for variable inductances, L, of a general nature. If R = 0, both equations show immediately that total flux is conserved. If R and L are given functions of the time, then both Eqs. (4.8) and (4.9) may be reduced to quadrature as follows. From Eq. (4.8), we have

$$\frac{d}{dt}\left[(L + L_1)\, I\right] + (L + L_1)\, I \frac{R}{L + L_1} = 0 \; ; \quad I(0) = 0 \quad .\text{(a)} \tag{4.10}$$

The solution to this equation is

$$I(t) = \frac{L_0 + L_1}{L + L_1} I_0 \exp\left(-\int_0^t \frac{R}{L + L_1}\, d\tau\right) \quad . \qquad \text{(a)} \tag{4.11}$$

By adding $I_{10}R$ to both sides of eq. (4.9), we obtain

$$\frac{d}{dt}\left[(L + L_1)\,(I + I_{10})\right] + (L + L_1)\,(I + I_{10})\,\frac{R}{L + L_1} = I_{10}R\ ;$$

$$I(0) = 0\ . \qquad \text{(b)} \qquad (4.12)$$

The solution to this equation is

$$I + I_{10} = \frac{L_0 + L_1}{L + L_1}\, I_{10}\, \exp\left(-\int_0^t \frac{R\,d\tau}{L + L_1}\right)$$

$$\times \left[1 + \frac{1}{L_0 + L_1}\int_0^t R\,d\tau\, \exp\left(\int_0^\tau \frac{R}{L + L_1}\,dz\right)\right]\ .\text{(b)} \qquad (4.13)$$

For case (a), the cavity field is proportional to the current I flowing through the system. For case (b), the cavity field is proportional to $I + I_{10}$, although only the current I flows in the external circuit. It is seen that the cavity field amplification for case (b) exceeds that for case (a) by the factor included in the bracketed expression of Eq. (4.13). If there is no resistance in the circuit, the cavity field amplifications are the same. An analogous relationship will be noted in Sec. 5, where the corresponding problem is treated by diffusion methods. Here, one of the problems considered is the determination of the maximum possible field amplification within a cavity (no external inductance). It also turns out there that somewhat higher amplifications arise when the initial flux is supplied by an external field instead of from an initial current. The reason for this is clearly associated with the larger resistive losses that occur when the fields arise solely from currents. (There is no resistive loss penalty associated with the initial magnetic field produced by an external source.)

The situation is different for powering the external load, L_1. Here we are only interested in the external current, I. For the lossless case, R = 0, the current I for case (a) exceeds that for case (b), and thus more energy will be delivered to L_1 for this case. The explanation for this is that in case (a), both cavity and load, L_1, contain initial flux, but in case (b), only the cavity has initial flux.

4.2 Constant Slab Velocity Solution

We continue this section by integrating Eq. (4.11) for the special case where R is constant, and the slab plates move with constant velocity v. The slabs collide at time $\tau = x_0/v$, usually called the generator "burnout time" because flux compression is then finished:

$$L = \frac{\mu \ell}{w} 2(x_0 - vt) = L_0\left(1 - \frac{t}{\tau}\right) . \tag{4.14}$$

Substitution of this expression into Eq. (4.11) gives for the current ratio

$$\frac{I}{I_0} = \frac{1}{\left(1 - \frac{L_0}{L_0 + L_1}\frac{t}{\tau}\right)^{1-R\tau/L_0}} . \tag{4.15}$$

The maximum current multiplication occurs at $t = \tau$ and is

$$\frac{I_M}{I_0} = \left(\frac{L_0 + L_1}{L_1}\right)^{1-R\tau/L_0} . \tag{4.16}$$

When $R = 0$, Eq. (4.16) shows that flux is conserved. When $R \neq 0$, Eq. (4.16) shows that maximum current amplification is reduced and that if $R\tau/L_0 = 1$, there is no current amplification. If $R\tau/L_0 > 1$, the initial current actually decays. We shall find somewhat similar behavior exhibited in the analogous diffusion equation solutions. However, we note that when the load L_1 gets very small, a legitimate situation in the lumped circuit model, the peak current gets very large when $R\tau/L_0<1$ and, conversely, gets very small when $R\tau/L_0>1$. This anomaly disappears when diffusion is taken into account.

4.3 Constant Slab Velocity; Approximate Diffusion Term

We can approximate diffusion into the plates, within the framework of the lumped parameter model, by adding a skin layer inductance term that varies as the square root of the time:

$$L(t) = L_0 \left[1 - \frac{t}{\tau} + 2a \left(\frac{t}{\tau}\right)^{1/2}\right] \quad . \tag{4.17}$$

Here, a is the ratio of skin inductance at burnout to the initial cavity inductance, or equivalently, the skin depth at burnout divided by the initial plate separation.

When the load is a pure resistance, R, ($L_1 = 0$), and the flux is only from a current, I, the equation for the current is

$$\frac{d}{dt}\left(L(t)I\right) + IR = 0; \; I(0) = I_0 \quad . \tag{4.18}$$

The solution to this equation is

$$\frac{I(t)}{I_0} = \left| \frac{1-T^{1/2}(\sqrt{a^2+1}-a)}{1+T^{1/2}(\sqrt{a^2+1}+a)} \right| \bullet \frac{R\tau a/L_0\sqrt{a^2+1}}{\left[1-T+2aT^{1/2}\right]^{1-R\tau/L_0}} \tag{4.19}$$

Here, we have used a reduced time variable $T = t/\tau$, which, at burnout, equals one.

We have plotted on Fig. 9 (solid curve) the current multiplication to burnout ($T = 1$) for the case where $RT/L_0 = 0.5$ and $a = 0.1$. We note from Eq. (4.17) that the initial inductance is L_0, which at burnout is $0.2L_0$. For comparison purposes, we show the solution for the corresponding problem with a fixed load inductance, whose solution is given by Eq. (4.15). In this case, to make the initial and final inductances the same, L_0 of Eq. (4.15) must be taken as $0.8\ L_0$ and $L_1 = 0.2\ L_0$ used in Eq. (4.17). It will be noted that the final current amplification is slightly smaller for this case. It is interesting to note that the current actually decreases slightly near the start of compression for the diffusion approximation solution. This happens because the inductance actually increases slightly at early times because the term with the square root of time initially overrides the term linear in time.

5. MOVING SLABS, CONSTANT CONDUCTIVITY

In this section we obtain solutions to several problems where semi-infinite slabs have constant conductivity and move together with constant velocity. In the first example there is no external load, in the other examples there are external loads in the circuit. In all cases, an initial current I_0 flows through the circuits. We will compare the results obtained for the first problem with previously published solutions for the case with no external load and with initial flux supplied from an external magnetic field source.

5.1 Summary of Previous Work

Paton and Millar[5] obtained the first solution to the moving slab diffusion problem, and our subsequent analysis of different problems in this section will parallel much of their work. They considered a cavity of total width x_0, filled with an initial magnetic field B_0. One slab was stationary, the other slab moved towards the fixed slab with constant velocity, v. Both slabs had fixed conductivity, σ. We cite one of their major conclusions. The maximum magnetic field multiplication, B_M/B_0, can be expressed in terms of a "magnetic Reynolds number" R as follows:

$$R = \mu\sigma\, x_0\, v \quad , \text{ and} \tag{5.1}$$

$$\frac{B_M}{B_0} = 1 + \frac{R}{8} + \sqrt{R/\pi} \quad . \tag{5.2}$$

Lehner, Linhart, and Somon[6] published a solution somewhat later which was more amenable to numerical calculation, particularly if the slab walls were of finite thickness instead of being infinitely thick as treated by Paton and Milar and, for the most part, in the analytic solutions given in this report. They gave the solution for the maximum magnetic field compression, B_M/B_0, for the following problem. Two infinite slabs initially separated by a distance

$2x_0$ contain an initial uniform magnetic field B_0. Both slabs move toward each other, each with a constant velocity, v. The maximum compression is again obtained in terms of a magnetic Reynolds number, R:

$$R = \mu\sigma\, x_0\, v \quad , \text{ and} \tag{5.3}$$

$$\frac{B_M}{B_0} = 1 + \frac{R}{2} + 2\sqrt{R/\pi} \quad . \tag{5.4}$$

It will be noted that the Reynolds number of Eq. (5.3) is defined in terms of half the cavity width, x_0, and half the relative plate velocity, v. Had R been defined in terms of total cavity width, $2x_0$, and total relative velocity, 2v, as in Eq. (5.1), then R in Eq. (5.4) would be reduced by a factor of four. The maximum compression predicted by Eq. (5.4) then would be the same as that given by Eq. (5.2).

5.2 Initial Current Source, No External Load

The slab boundary condition is again given by Eq. (2.26). Here, $V_{ext} = 0$, and we can write a general flux term as follows:

$$\phi = 2\ell\,(x_0 - vt)\,(B + B_{10}) \quad . \tag{5.5}$$

Here, B_{10} is an external impressed field, and B is the field that arises from a current $I = -wB/\mu$. The problem summarized in Sec. 5.1 is solved using this relation to determine the boundary condition. In that case, the initial cavity field term $B(0,0) = 0$ since there is no initial current. The initial field distribution in the slabs, however, is given by $B(x,0) = B_{10}$. Equation (5.5) is also applicable to the more general problem where both an externally impressed field and an initial current are present. We consider here, however, the case where only an initial current $I_0 = -wB_0/\mu$ flows in the system. Thus, $B_{10} = 0$. We are mainly interested in the magnetic fields and will, as before, cast the equations in terms of B, although the total current flowing can be obtained from the cavity field, B(0,t). In this case, the set of

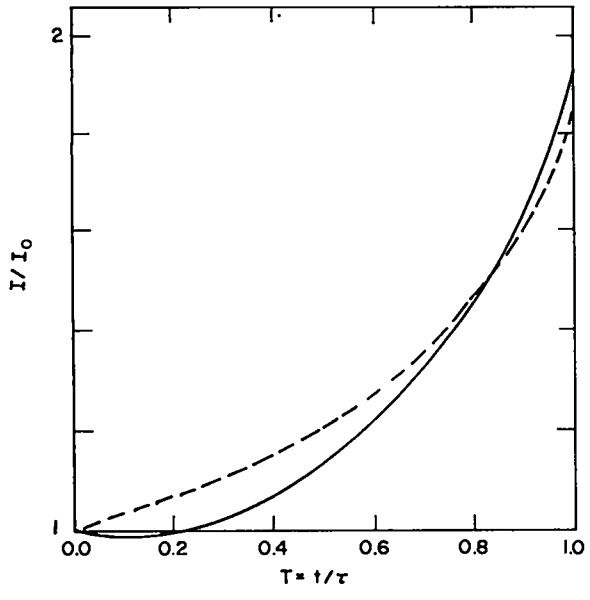

Fig. 9.
Current gains for a plate generator with resistance. An empirical diffusion term was used for the solid curve system.

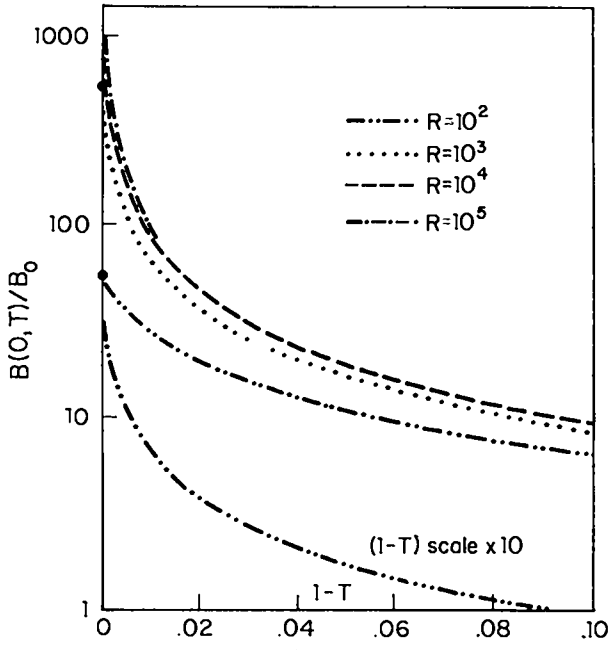

Fig. 10.
Cavity field compression ratios for various magnetic Reynolds numbers. Reduced times T are plotted from burnout.

Eqs. (3.1)-(3.5) apply except the boundary condition, Eq. (3.2), which is now replaced by

$$-\frac{d}{dt}\left[2\ell\,(x_0 - vt)\,B(0,t)\right] + \frac{2\ell}{\mu\sigma}\left(\frac{\partial B}{\partial x}\right)_0 = 0 \quad . \tag{5.6}$$

Equation (5.6) can be expressed in terms of the generator burnout time τ of Eq. (4.14) to

$$-\frac{d}{dt}\left[\left(1 - \frac{t}{\tau}\right) B(0,t)\right] + \frac{1}{\mu\sigma x_0}\left(\frac{\partial B}{\partial x}\right)_0 = 0 \quad . \tag{5.7}$$

Upon differentiating, the boundary condition becomes

$$-\frac{dB(0,t)}{dt} + \frac{B(0,t)}{\tau} + \frac{t}{\tau}\frac{dB(0,t)}{dt} + \frac{1}{\mu\sigma x_0}\left(\frac{\partial B}{\partial x}\right)_0 = 0 \quad . \tag{5.8}$$

The Laplace transform solution follows that given in Sec. 3.1 through Eqs. (3.1), (3.3), and (3.5) to yield

$$\beta(x,s) = A(s)\exp\left(-x\sqrt{\mu\sigma s}\right) \quad . \tag{5.9}$$

To proceed further, we transform Eq. (5.8):

$$-\int_0^\infty \frac{dB(0,t)}{dt} e^{-st}\,dt + \int_0^\infty \frac{B(0,t)}{\tau} e^{-st}\,dt + \frac{1}{\tau}\int_0^\infty t\, e^{-st}\frac{dB(0,t)}{dt}\,dt + \frac{1}{\mu\sigma x_0}\frac{\partial}{\partial x}\int_0^\infty B\, e^{-st}\,dt\,\Big|_0 = 0 \quad . \tag{5.10}$$

From Ref. 9[Eq. (30), p. 6, n = 1], the transform of the third term is given by

$$\frac{1}{\tau}\int_0^\infty t\, e^{-st}\frac{dB(0,t)}{dt}\,dt = -\frac{1}{\tau}\frac{d}{ds}\left(s\,\beta(x,s)\right)\Big|_{x=0} \quad . \tag{5.11}$$

With the use of this relation and the initial condition, $B(0,0) = B_0$, Eq. (5.10) becomes

$$B_0 - s\beta(0,s) - \frac{s}{\tau}\left(\frac{d\beta}{ds}\right)_{x=0} + \frac{1}{\mu\sigma x_0}\left(\frac{d\beta}{dx}\right)_0 = 0 \quad . \tag{5.12}$$

Substitution of Eq. (5.9) into Eq. (5.12) leads to the following differential equation for A(s):

$$\frac{dA(s)}{ds} + A\left(\tau + \frac{\tau}{x_0\sqrt{\mu\sigma s}}\right) = \frac{B_0\tau}{s} \quad . \tag{5.13}$$

Equation (5.13) can be written as

$$\frac{d}{ds}\left[A(s)\exp\left(\tau s + \frac{2\tau s^{1/2}}{x_0\sqrt{\mu\sigma}}\right)\right] = \frac{B_0\tau}{s}\exp\left(\tau s + \frac{2\tau s^{1/2}}{x_0\sqrt{\mu\sigma}}\right) \quad . \tag{5.14}$$

The right-hand expression contains singularities at s = 0. Paton and Milar[5] subtract terms from both sides of their analogous equation to obtain a solution regular at s = 0. We will not do this here because, as it turns out, these terms do not contribute to our solution. The expression for A(s) then becomes

$$A(s) = \exp\left(-\tau s - \frac{2\tau s^{1/2}}{x_0\sqrt{\mu\sigma}}\right)\left[k + \int_{(0)}^{s}\frac{B_0\tau}{\xi}\exp\left(\tau\xi + \frac{2\tau\xi^{1/2}}{x_0\sqrt{\mu\sigma}}\right)d\xi\right] \quad . \tag{5.15}$$

We rewrite the second term of Eq. (5.15) as

$$\int_{(0)}^{s}\frac{B_0\tau}{\xi}\,d\xi\; e^{-\tau(s-\xi)-\frac{2\tau}{x_0\sqrt{\mu\sigma}}(s^{1/2}-\xi^{1/2})} \quad .$$

We then replace the integration variable ξ by ws. The limits on w then become 0 and 1. The bracketed expression then becomes

$$\int_{(0)}^{1} B_0\tau\,\frac{dw}{w}\; e^{-\tau s(1-w)-\frac{2\tau s^{1/2}}{x_0\sqrt{\mu\sigma}}(1-w^{1/2})} \quad .$$

The complete expression for $\beta(x,s)$ then becomes

$$\beta(x,s) = e^{-\sqrt{\mu\sigma s}\,x}\left[k\, e^{-\tau s - \frac{2\tau s^{1/2}}{x_0\sqrt{\mu\sigma}}}\right.$$

$$\left. + \int_{(0)}^{1} \frac{B_0\tau}{w}\, dw\, e^{-\tau s(1-w) - \frac{2\tau s^{1/2}}{x_0\sqrt{\mu\sigma}}(1-w^{1/2})}\right] . \qquad (5.16)$$

From Ref. 9 [Eq. (66), p. 175], the integral of a transform over a parametric variable has as its inverse the integral of the inverse transform over the same parametric variable. Using this relation with Eq. (5.16), we may write for B(x,t):

$$B(x,t) = \frac{1}{2\pi i} \int_{Br} k\, e^{s(t-\tau) - \frac{2\tau s^{1/2}}{x_0\sqrt{\mu\sigma}} - x\sqrt{\mu\sigma s}} + \int_{(0)}^{1} \frac{dw}{w}$$

$$\times \frac{1}{2\pi i} \int_{Br} B_0\tau\, e^{s[t-\tau(1-w)] - \frac{2\tau s^{1/2}}{x_0\sqrt{\mu\sigma}}(1-w^{1/2}) - \sqrt{\mu\sigma s}\,x} . \qquad (5.17)$$

At this point we make use of the well-known result that the transform of a function $g(s)e^{-\alpha s}$ is the transform of g(s) delayed in time by α, or

$$L^{-1}\left[g(s)\, e^{-\alpha s}\right] = 0 ; \quad t < \alpha$$

$$= f(t-\alpha) ; \quad t \geq \alpha . \qquad (5.18)$$

The first term in Eq. (5.18) does not contribute to the solution for we are only interested in times $t \leq \tau$, and according to Eq. (5.17), the inverse transform of the remaining integral is zero up to this time. It may be remarked here that the various terms we should have added to Eq. (5.15) to make the expression A(s) nonsingular at s = 0 all drop out for the same reason. They, too, give rise to terms that contribute only for $t \geq \tau$.

There remain for B(x,t) contributions only from the second expression. These contributions exist only for $t \geq \tau(1-w)$ or $w \geq 1 - t/\tau$. The solution for B(x,t) then becomes

$$B(x,t) = B_0\tau \int_{1-t/\tau}^{1} \frac{dw}{w}$$

$$L^{-1}\left\{e^{-s^{1/2}\left[\frac{2\tau}{x_0\sqrt{\mu\sigma}}(1-w^{1/2})+x\sqrt{\mu\sigma}\right]}\right\}_{t\to t-\tau(1-w)} \quad . \tag{5.19}$$

From Ref. 9, [Eq. (14), p. 246],

$$B(x,t) = \frac{B_0\tau}{2\sqrt{\pi}} \int_{1-t/\tau}^{1} \frac{dw}{w} \frac{\frac{2\tau}{x_0\sqrt{\mu\sigma}}(1-w^{1/2})+ x\sqrt{\mu\sigma}}{[t - \tau(1-w)]^{3/2}}$$

$$\times e^{-\left(\frac{\left[\frac{2\tau}{x_0\sqrt{\mu\sigma}}(1-w^{1/2})+x\sqrt{\mu\sigma}\right]^2}{4[t-(1-w)\tau]}\right)} \quad . \tag{5.20}$$

We are mainly interested in the cavity field which then also gives the total current. Equation (5.20), at x = 0, with the definitions given below, reduces to

$$B(0,t) = \frac{B_0}{\sqrt{\pi R}} \int_{1-T}^{1} \frac{dw}{w} \frac{1 - w^{1/2}}{[T - (1-w)]^{3/2}} e^{-\frac{(1-w^{1/2})^2}{R[T - (1-w)]}} \quad . \tag{5.21}$$

$$T = \frac{t}{\tau} \; ; \quad R = \mu\sigma v x_0 \; ; \quad v = \frac{x_0}{\tau} \quad . \tag{5.22}$$

At burnout, $t = \tau$, $T = 1$, and Eq. (5.21) reduces to

$$\frac{B(0,\tau)}{B_0} = \frac{1}{\sqrt{\pi R}} \int_0^1 \frac{dw}{w^{5/2}} (1-w^{1/2})\, e^{-\frac{(1-w^{1/2})^2}{Rw}} \quad . \tag{5.23}$$

Upon substituting $y = 1/\sqrt{w} - 1$, Eq. (5.23) becomes

$$\frac{B(0,\tau)}{B_0} = \frac{2}{\sqrt{\pi R}} \int_0^\infty y(y+1)\, e^{-y^2/R}\, dy \quad . \tag{5.24}$$

This expression reduces to

$$\frac{B(0,\tau)}{B_0} = \frac{R}{2} + \sqrt{R/\pi} \quad . \tag{5.25}$$

Equation (5.25) may be compared with Equation (5.4), which gives the limiting cavity field compression when the initial flux is supplied from an external magnetic field, B_0. If the Reynolds number R is large, both expressions tend to a limiting compression R/2. When initial flux is supplied by an external field, even with very small values of R, the final field cannot be less than the initial field. Consequently, the final compression cannot be less than one, as seen from Eq. (5.4). However, when the initial flux is produced by an initial current, as in this example, if R is small enough, the current can dissipate to such an extent that the final compression is less than unity. From Eq. (5.25), we find that the amplification is unity for $R = 2\left(1 + 1/\pi - \sqrt{[1+(1/\pi)]^2 - 1}\right) = 0.9186$. If R is greater than 0.9186, the final field will be amplified; if it is less, the final field will be less than the initial field. Equation (5.25) also readily yields the value of the skin depth at burnout. Since all of the initial flux now resides in the skin, $2\ell x_0 B_0 = 2\ell D_{sk} B(\tau)$ and $D_{sk} = x_0 B_0 / B(\tau)$, or from Eq. (5.22),

$$D_{sk} = \frac{x_0}{R/2 + \sqrt{R/\pi}} = \frac{2}{\mu\sigma v + 2(\mu\sigma v/\pi x_0)^{1/2}} \quad .$$

This situation may be compared to that obtained for the lumped parameter treatment. From Eq. (4.16), it is clear that $L_0/R\tau$ (here, R is the plate resistance) plays the role of a Reynolds number. Unless $L_0/R\tau > 1$, no

amplification results. However, the analogy breaks down when we equate the two expressions for the Reynolds number. The effective skin depth for plate resistance must be taken to be x_0, half the cavity width.

Equation (5.21) has been integrated numerically for various values of R and T, and these are plotted on Fig. 10. Curves of compression vs. 1-T are given for the latter stages of compression (T from 0.86 to 1.0) for values of R = 10^2, 10^3, 10^4, and 10^5. If the plates were perfectly conducting and σ and R infinite, the theoretical compression would be given by

$$\frac{B(0,T)}{B_0} = \frac{1}{1 - T} .$$

Inspection of Fig. 10 shows that most of the compression occurs near burnout, T = 1, particularly for large Reynolds numbers. Experimentally, compression of the plates is normally achieved by use of explosives. It is clear that a high degree of simultaneity in explosive initiation and detonation is called for if large compression ratios are to be achieved. Further, the metal plates must be of uniform thickness and density and must be carefully aligned. These conditions are relaxed somewhat when the plate generator is used to deliver energy to an external cavity, the problem taken up in Sec. 5.3.

5.3 Initial Current Source, External Load L_1

The slab boundary condition for this case Eq. (2.26) now includes an external potential term, $L_1\, dI/dt$, which we cast in terms of the cavity field:

$$V_{ext} = L_1 \frac{dI}{dt} = - \frac{w}{\mu} L_1 \frac{dB(0,t)}{dt} . \qquad (5.26)$$

Addition of this term to Eq. (5.6) gives as the boundary condition for this example

$$- \frac{d}{dt} \left\{ \left[2\ell \, (x_0 - vt) + \frac{w}{\mu} L_1 \right] B(0,t) \right\} + \frac{2\ell}{\mu\sigma} \left(\frac{\partial B}{\partial x} \right)_0 = 0 . \qquad (5.27)$$

Equation (5.27) can be written in terms of the cavity inductance, L_0, as follows:

$$-\frac{d}{dt}\left[\left(1-\frac{t}{\tau_{eff}}\right)B(0,t)\right]+\frac{1}{\mu\sigma x_0}\,\frac{L_0}{L_0+L_1}\left(\frac{\partial B}{\partial x}\right)_0=0\quad, \tag{5.28}$$

where

$$\tau_{eff}=\frac{x_0}{v}\,\frac{L_0+L_1}{L_0}=\tau\,\frac{L_0+L_1}{L_0}\quad. \tag{5.29}$$

This equation is completely equivalent to Eq. (5.7) except where the parameter x_0 occurs. It should be replaced by the quantity a, given below:

$$a=x_0\,\frac{L_0+L_1}{L_0}\quad. \tag{5.30}$$

In particular, Eqs: (5:21) and (5:22) can be taken over directly:

$$B(0,t)=\frac{B_0}{\sqrt{\pi R_{eff}}}\int_{1-T_{eff}}^{1}\frac{dw}{w}\,\frac{1-w^{1/2}}{\left[T_{eff}-(1-w)\right]^{3/2}}\times e^{-\frac{(1-w^{1/2})^2}{R_{eff}\left[T_{eff}-(1-w)\right]}}\quad, \tag{5.31}$$

where

$$R_{eff}=\mu\sigma va=\mu\sigma v x_0\,\frac{L_0+L_1}{L_0}\quad,\ \text{and} \tag{5.32}$$

$$T_{eff} = \frac{t}{\tau_{eff}} \quad . \tag{5.33}$$

An immediate consequence of these equations is that the maximum field multiplication is reduced over that obtained when there is no external load. At burnout $T_{eff} = L_0/(L_0 + L_1)$. Thus the lower integration limit of Eq. (5.31) is $L_1/(L_0 + L_1)$ instead of zero as is the case for Eq. (5.21).

Ratios $B(T)/B_0$ are plotted against $1 - T_{eff}$ for various values of R_{eff} on Fig. 11. Values were obtained by numerical integration of Eq. (5.31), which, with appropriate relabeling, is the same integral of Eq. (5.21). For plate generators, L_0 is usually only a few tenths of a microhenry. Consequently, it is seldom that external loads, L_1, are small enough to make the limiting compression ratio exceed 100. Therefore, the ordinates of Fig. 11 are plotted over only two orders of magnitude, and the compression curves lend themselves well to log-log plots.

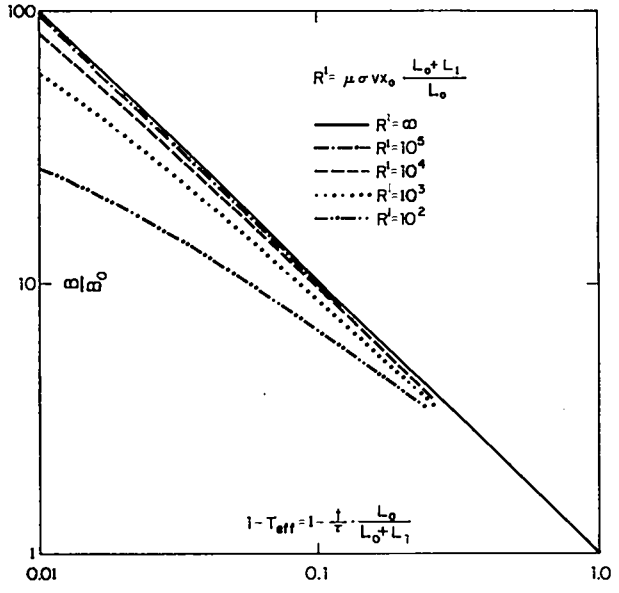

Fig. 11.
Cavity field compression ratios for various magnetic Reynolds numbers with external inductance L_1.

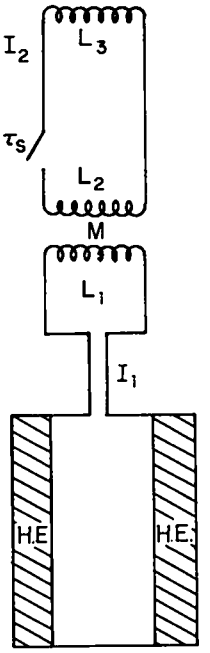

Fig. 12.
Two-loop external circuit connected to a plate generator. The loops are transformer coupled.

When $R_{eff} = \infty$ (perfect conductivity), flux is conserved, and the field compression ratio is given by

$$\frac{B(T)}{B_0} = \frac{L_0 + L_1}{L(t) + L_1} = \frac{L_0 + L_1}{L_0\left(1 - \frac{t}{t}\right) + L_1} = \frac{1}{1 - \frac{t}{\tau_{eff}}} = \frac{1}{1 - T_{eff}} \quad . \tag{5.34}$$

The curve on Fig. 11 for $R_{eff} = \infty$ is therefore a straight line of slope -1. Curves for finite values of R_{eff} show lesser values of compression for the same value of $(1 - T_{eff})$. As an example of the use of Fig. 11, take

$$R_{eff} = 1000 \; ; \quad \frac{L_0}{L_0 + L_1} = 0.9 \quad .$$

At burnout, $1 - T_{eff} = 1 - 0.9 = 0.1$. Reading from the graph on the $R_{eff} = 1000$ curve, field multiplication at burnout is 8.70.

At a time $t = 0.95\tau$, we have

$$1 - T_{eff} = 1 - (0.95)\,(0.9) = 0.145 \quad .$$

The compression at this stage of generation is 6.15, approximately 70% of maximum compression. This result illustrates a practical situation of great importance in generator design. If this example was based upon an actual design in which a field (or current) amplification of 8.70 were required, then it is clear that if compression to the load L_1 were stopped 5% early in time for some reason, the actual compression would be substantially reduced over the design value. In many of our applications, generator burnout times are only a few microseconds. It is clear that loss of only a few tenths of a microsecond of compression can be serious. This situation is aggravated when the ratio $(L_0 + L_1)/L_1$ is larger. The extreme case occurs when $L_1 = 0$, that is, no external load. Reference to Fig. 10 shows that maximum compression at burnout

(1 - T = 0) is 520 for R = 1000. At $t/\tau = 0.95$, the compression ratio is only 16, or about 3% of that for complete compression!

Figure 11 also allows computation of the skin depth at burnout since the initial flux now resides entirely in the generator plate skins and the external load, L_1:

$$D_{sk} = x_0 \left[\frac{L_0+L_1}{L_0}\frac{B_0}{B_M} - \frac{L_1}{L_0}\right] \quad .$$

For the example discussed above, R_{eff}=1000, $L_0/(L_0+L_1) = 0.9$, the field magnification at burnout was 8.70. Using $(L_0+L_1)/L_0 = 1.111$ and $L_1/L_0 = 0.111$, we obtain

$$D_{sk} = 0.0166x_0 \quad .$$

When L_1/L_0 is small, the flux loss in the skin is larger. Consider R_{eff}=1000, $L_0/(L_0+L_1) = 0.99$. From Fig. 11, $B_M/B_0 = 61.2$. With $(L_0+L_1)/L_0 = 1.0101$ and $L_1/L_0 = 0.0101$, the skin depth is found to be

$$D_{sk} = 0.0064x_0 \quad .$$

The skin depth is smaller in this case, but the skin flux is larger since the final field is greater. The flux losses for the two cases can be compared by multiplying the skin depths by the field compression factors. The ratio of these numbers for the two cases is (0.0064)(61.2)/(0.0166)(8.70) = 2.71.

5.4 Initial Current Source, Transformer Coupling to Load

Figure 12 shows a plate generator driving an external inductance L_1. The external load to be energized, L_3, is in turn transformer-coupled to L_1 through the secondary coil, L_2. The mutual inductance is M.

In practice, use of a switch, τ_s, which can delay connection of the secondary circuit, allows considerable versatility in the control of the current pulse shape through the load L_3. However, incorporation of this feature in the analysis greatly complicates the diffusion analysis. Instead, we assume the switch is closed at time t = 0 when the generator motion starts. The initial currents are then $I_1(0) = I_0$ for the initial slab surface current, and $I_2(0) = 0$.

The external potential for the generator circuit and the secondary circuit equation are

$$V_{ext} = L_1 \frac{dI_1}{dt} + M \frac{dI_2}{dt} \quad , \text{ and} \tag{5.35}$$

$$M \frac{dI_1}{dt} + (L_2 + L_3) \frac{dI_2}{dt} = 0 \quad . \tag{5.36}$$

Equation (5.36) can be used to eliminate dI_2/dt in V_{ext} and can also be integrated directly to give I_2 in terms of I_1:

$$I_2 = \frac{-M}{L_2 + L_3} (I_1(t) - I_0) \quad , \text{ and} \tag{5.37}$$

$$V_{ext} = L_1' \frac{dI_1}{dt} \; ; \quad L_1' = L_1 - \frac{M^2}{L_2 + L_3} \quad . \tag{5.38}$$

Comparison of Eq. (5.38) with Eq. (5.26) shows that this problem reduces exactly to that for an external load, L_1 above, with the substitution of the effective inductance L_1' for L_1. The current I_2 may then be obtained from I_1 or from the cavity field as in Eq. (5.26).

If the coupling of L_1 and L_2 can be maintained closely, the use of transformers greatly increases the use of generators in that it allows them to energize loads of much greater inductance than that of the generator. Although

we will not demonstrate it here, transformers also allow energizing other types of impedances such as resistances and capacitances that would not be possible if they were series coupled to the generator. Most of these examples can be readily demonstrated by the lumped parameter treatment outlined in Sec. 4.

As an example let us take a plate generator of initial inductance L_0 = 0.1 μH which is to energize a load L_3 = 1 μH. If L_3 were in series with the generator, even in the lossless case the maximum energy multiplication factor would be $(L_0 + L_1)/L_1 = (0.1 + 1)/1 = 1.1$. We now consider use of a transformer and take L_1 = 0.01 μH and L_2 = 4 μH. For a coupling coefficient of 0.9, $M = 0.9\ (L_1\ L_2)^{1/2}$ = 0.18 μH. We note on Fig. 11 that the maximum cavity field or primary current multiplication is determined by the ordinate value of $L_1'/(L_0 + L_1')$ for a given Reynolds number R'. From Eq. (5.38), we find

$$L_1' = 0.01 - \frac{(0.18)^2}{5} = 0.00352 \ \mu H \quad , \text{ and}$$

$$\frac{L_1'}{L_0 + L_1'} = \frac{0.00352}{0.10352} = 0.0340 \quad .$$

For $R' = 1000$, the primary current multiplication is read from Fig. 11 as 22.9. If we set I_0 = 1 MA, then from Eq. (5.37), the maximum value of I_2 is

$$I_{2(max)} = -\frac{0.18}{5}\ (21.9)\ MA = -0.788\ MA.$$

The initial energy in the circuit and the final energy stored in L_3 are

$$E_0 = \frac{1}{2}\ (0.1 + 0.01)\ 10^{-6} \times (10^6)^2 = 55\ kJ \quad ,$$

$$E(Load,\ Max) = \frac{1}{2}\ (1)\ 10^{-6} \times (0.788 \times 10^6)^2 = 310\ kJ, \text{ and}$$

$$\frac{E(load,\ Max)}{E_0} = 5.6 \quad .$$

If the example is repeated with very good coupling, k = 0.98, (M = 0.196 μH), the maximum load current is 1.22 MA and the stored load energy is 744 kJ, or 13.5 times the initial circuit energy. On the other hand, if k is reduced to 0.8 (M = 0.16 μH), the maximum load energy is only 139 kJ, an energy multiplication factor of about 2.5. It may be noted from Fig. 11 that the energy gain developed in the primary coil alone (no transformer) is only 6.6. The reason for the high energy gain for the tight-coupling cases is that the generator behaves as though it were feeding a series inductance L_1' whose value is reduced over that of the true primary inductance L_1. The better the transformer coupling, the smaller the effective inductance.

5.5 Initial Current Source, External Load, R

For this case, the external potential of Eq. (2.26) is IR. Replacing I by the cavity field - B(0,t) w/μ, with $\phi = 2\ell(x_0 - vt)\, B(0,t)$ for the cavity flux, Eq. (2.26) becomes

$$\frac{-dB(0,t)}{dt} + \frac{t}{\tau}\frac{dB(0,t)}{dt} + \frac{B(0,t)}{\tau} - \frac{R}{L_0}B(0,t) + \frac{1}{\mu\sigma x_0}\left(\frac{\partial B}{\partial x}\right)_0 = 0 \qquad (5.39)$$

From Ref. 9 [Eq. (30), p 6], the transform of the second term is

$$\frac{-d(s\beta)}{ds}/\tau .$$

The transform of Eq. (5.39), after some manipulations, gives the boundary condition

$$\frac{d\beta}{ds} + \beta\left[\tau + \frac{R\tau}{L_0 s}\right] - \frac{\tau}{\mu\sigma x_0 s}\left(\frac{d\beta}{dx}\right)_0 = B(0,0)\tau/s \quad . \qquad (5.40)$$

As in the other examples, β(x,s) is given by Eq. (5.9). Substitution of this expression into Eq. (5.40) leads to the following equation for A(s):

$$\frac{dA}{ds} + A\left[\tau + \frac{R\tau}{L_0 s} + \frac{1}{x_0\sqrt{\mu\sigma s}}\right] = \frac{B(0,0)\tau}{s} \quad . \tag{5.41}$$

The solution for A(s) is

$$A = \frac{-R\tau}{L_0} \exp(-\tau s - 2\tau s^{1/2}/x_0\sqrt{\mu\sigma})\left[k + \int_{(0)}^{s} B(0,0)\tau\xi^{R\tau/L_0 - 1}\, d\xi \exp(\tau\xi + 2\tau\xi^{1/2}/x_0\sqrt{\mu\sigma})\right] \quad .(5.42)$$

Following the procedure of the previous examples, we see that only the second bracketed term of Eq. (5.42) contributes for $t<\tau$. At this point we take $x = 0$, and solve only for the cavity field. Setting $\xi = Ws$, we obtain

$$\frac{B(0,t)}{B(0,0)} = \frac{\tau}{2\pi i}\int_{(0)}^{1}\frac{dW}{W}\, W^{\frac{R\tau}{L_0}}\int_{Br} ds\, \exp\left[s[t-\tau(1-W)] - 2\tau s^{1/2}(1-W^{1/2})/x_0\sqrt{\mu\sigma}\right] \quad .(5.43)$$

We replace the contour integral by the transform of the latter exponential term displaced in time to $t - \tau(1-W)$, as in Sec. 5.2, and obtain

$$\frac{B(0,t)}{B(0,0)} = \tau\int_{1-\epsilon/\tau}^{1} dW\, W^{\frac{R\tau}{L_0}-1}\left[\frac{2\tau(1-W^{1/2})\exp\left\{-\left(2\tau(1-W^{1/2})/x_0\sqrt{\mu\sigma}\right)^2/4[t-\tau(1-W)\right\}}{x_0\sqrt{\mu\sigma}\qquad 2\sqrt{\pi}\,[t-\tau(1-W)]^{3/2}}\right] \quad .(5.44)$$

With the substitution $Z = W^{-1/2} - 1$, we obtain the limiting cavity field at burnout, $t=\tau$:

$$\frac{B(0,\tau)}{B(0,0)} = \frac{2}{\sqrt{\pi R}}\int_0^{\infty} Z dZ (1+Z)^{1-2R\tau/L_0} \exp(-Z^2/R) \quad . \tag{5.45}$$

As before, the Reynolds number R is defined as follows:

$$R = \mu\sigma v x_0; \; v = x_0/\tau \quad . \tag{5.46}$$

Eq. (5.45) can be expressed in terms of tabulated functions for integral values of $2R\tau/L_0$. For the particular case $R\tau/L_0 = 0.5$, we readily obtain

$$\frac{B(0,\tau)}{B(0,0)} = \sqrt{R/\pi}; \; R\tau/L_0 = 0.5 \quad . \tag{5.47}$$

We can compare this with the lumped parameter solution, Eq. (4,19), plotted on Fig. 9 for $R\tau//L_0 = 0.5$, a = 0.1. The current amplification was only about 2 for this case. From Eq. (5.47), R~12 to match this case, a very small value for explosive-driven systems. We note finally that $\sqrt{R/\pi}$ is, to within a factor of order unity, x_0/τ skin. As is often found, attempts to correlate skin depths from the lumped parameter model are not very good. This is the case here, although the skin depth taken for the lumped circuit solution was $0.1(2x_0)$ and that required from Eq. (5.47) is several times larger.

5.6 Mixed Initial Field and Current Sources

The examples considered here have had an initial surface current I_0 as the original source of magnetic flux. Most of them can also be solved if the initial energy comes from an impressed external field, B_{10}, or a mixture of the two sources. In the latter case, the flux term entering the boundary condition, Eq. (2.26), is given by Eq. (5.5). The major analytic differences in the problem of Sec. 5.2 (no external load) occurs in Eq. (5.13). If the initial energy source is from an externally impressed field, the right-hand side of the equation contains a term in $1/s^2$ instead of 1/s. The Laplace inversion then gives the cavity field as an integral of the error function[5] instead of Eq. (5.21). If the initial energy source is mixed, then the cavity field is expressed in terms of both solutions. The limiting compression that can be obtained is then weighted appropriately between the values given in Eqs. (5.2) and (5.25).

ACKNOWLEDGMENTS

I am greatly indebted to a number of people. My colleagues Wray B. Garn, Dennis J. Erickson, Bruce L. Freeman and Dennis R. Peterson have all influenced my thoughts on this subject in one way or another. In particular, I have benefited greatly from extensive discussions with Robert S. Caird on many of the topics considered. Admirable calculational support was furnished by Rose Mary Boicourt, particularly that required for Figs. 10 and 11. The not inconsiderable typing chores were initially handled in expert fashion by Phyllis Sullivan and Adele E. Zimmermann. The final, demanding task of putting the manuscript in publishable form was undertaken by Mary Ann Lucero to whom I owe special thanks.

APPENDIX

RECENT MATERIAL

The tendency of current to concentrate at the edges of good conductors was touched upon briefly in Sec. 2 and illustrated by Fig. 3. Recently, Kerrisk[11] has published work on the distribution of currents in conductors at high frequencies. This work convincingly demonstrates the current concentration effect.

The author only recently became aware of a paper by Bichenkov[12] that treats the compression of a cavity field by two semi-infinite slabs in which the initial flux is generated by a current. This is the example treated in Sec. 5.2 of this report. The limiting compression ratio given is equivalent to our Eq. (5.25), although Bichenkov uses a parameter that is the inverse square of our Reynolds number. The method of solution follows that of Lehner, Linhart, and Somon.[6] Since both papers were published in 1964, it is difficult to say which has precedence. In any event, no external loads were attached to the cavities, which is a major point of departure of the present work.

REFERENCES

1. C. M. Fowler, R. S. Caird, and W. B. Garn, "An Introduction to Explosive Magnetic Flux Compression Generators," Los Alamos Scientific Laboratory Report LA-5890-MS (March 1975).

2. C. M. Fowler, R. S. Caird, W. B. Garn and D. B. Thomson, "Flux Concentration by Implosion," in High Magnetic Fields, H. Kolm, B. Lax, F. Bitter and R. Mills, Eds. (The MIT Press, Massachusetts Institute of Technology and John Wiley and Sons, Inc., New York, 1962), Chap. 25, pp. 269-276.

3. R. S. Caird, C. M. Fowler, D. J. Erickson, B. L. Freeman, and W. B. Garn, "A Survey of Recent Work on Explosive-Driven Magnetic Flux Compression Generators," in Energy Storage, Compression and Switching, Vol. 2, V. Nardi, H. Sahlin, and W. H. Bostick, Eds. (Plenum Publishing Corp., 1983), pp. 1-18.

4. H. Knoepfel, Pulsed High Magnetic Fields, (North-Holland Publishing Co., Amsterdam-London, and American Elsevier Publishing Co., Inc., New York, 1970), Chap. 3, pp. 46-72.

5. A. Paton and W. Millar, "Compression of Magnetic Field Between Two Semi-Infinite Slabs of Constant Conductivity," J. Appl. Phys. 35, (4), 1141-1146 (1964).

6. G. Lehner, J. G. Linhart, and J. P. Somon, "Limitations on Magnetic Fields Obtained by Flux-Compression: I," Nucl. Fus. 4, pp. 362-379 (1964).

7. C. M. Fowler, W. B. Garn, and R. S. Caird, "Production of Very High Magnetic Fields by Implosion," J. Appl. Phys. 31, (3), 588-594 (1960).

8. F. E. Allison, "Diffusion of a Magnetic Field from a Gap Between Two Semi-Infinite Conductors," Ballistic Research Laboratories Memorandum No. 1662 (June 1965).

9. G. E. Roberts and H. Kaufman, Table of Laplace Transforms, (W. B. Saunders Co., Philadelphia and London, 1966).

10. M. Abramowitz and I. A. Stegun, Eds, Handbook of Mathematical Functions - with Formulas, Graphs, and Mathematical Tables (National Bureau of Standards Applied Mathematics Series • 55, 1964).

11. J. F. Kerrisk, "Current Distribution and Inductance Calculations for Railgun Conductors," Los Alamos National Laboratory Report LA-9092-MS (November 1981).

12. Ye. I. Bichenkov, "Effect of Finite Conductivity on Obtaining Strong Magnetic Fields by the Rapid Pressing of Conducting Shells," Zhurnal Prikladnoy Mekhaniki i Tekhnicheskoy Fiziki, Isd-vo "Nauka," Nr 6, pp. 3-5, (1964). English translation, Report FTD-ID(RS)I-1727-76, may be obtained from the Translation Division, Foreign Technology Division, Wright Patterson Air Force Base, Ohio.

☆U.S. GOVERNMENT PRINTING OFFICE: 1984-0-776-026/4024

Printed in the United States of America
Available from
National Technical Information Service
US Department of Commerce
5285 Port Royal Road
Springfield, VA 22161

Microfiche (A01)

Page Range	NTIS Price Code	Page Range	NTIS Price Code	Page Range	NTIS Price Code	Page Range	NTIS Price Code
001-025	A02	151-175	A08	301-325	A14	451-475	A20
026-050	A03	176-200	A09	326-350	A15	476-500	A21
051-075	A04	201-225	A10	351-375	A16	501-525	A22
076-100	A05	226-250	A11	376-400	A17	526-550	A23
101-125	A06	251-275	A12	401-425	A18	551-575	A24
126-150	A07	276-300	A13	426-450	A19	576-600	A25
						601-up*	A99

*Contact NTIS for a price quote.

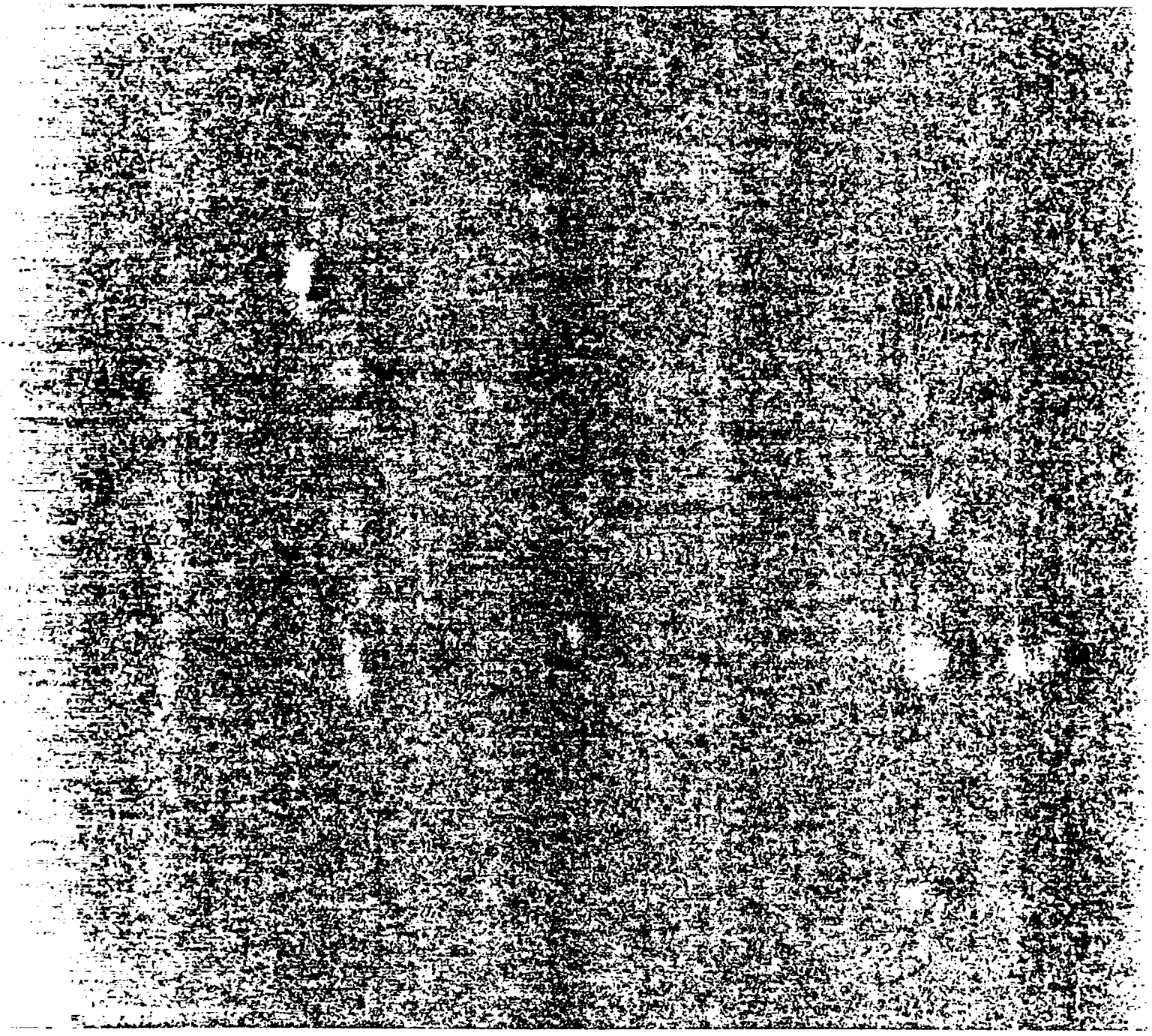

Los Alamos